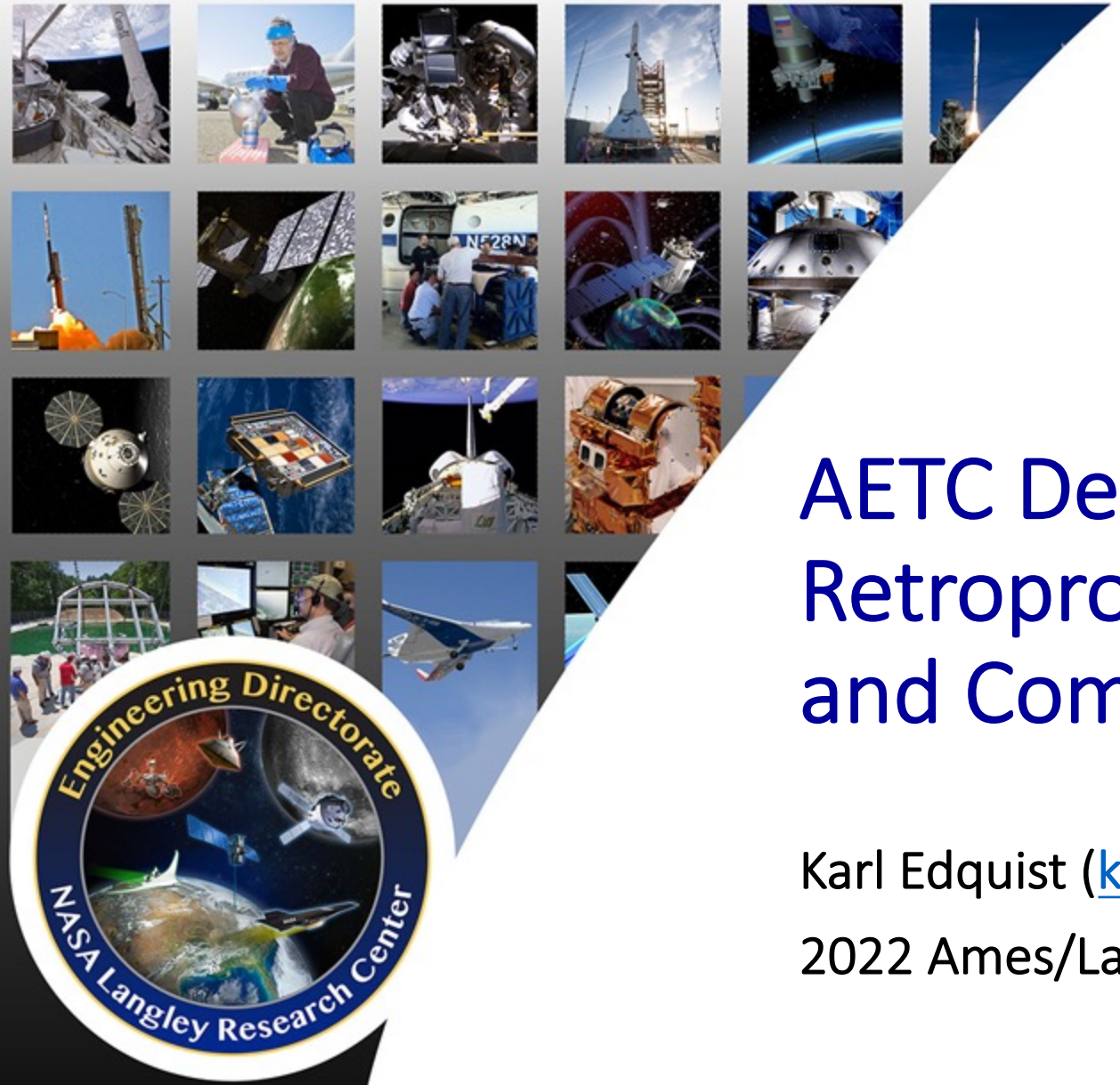

National Aeronautics and Space Administration

AETC Descent Systems Studies (AKA Retropropulsion Wind Tunnel Testing and Computational Flowfield Status)

Karl Edquist (karl.t.edquist@nasa.gov)

2022 Ames/Langley EDL Summer Seminar

11 July 2022

Background & Motivation

- **NASA studies show that powered descent starting at supersonic conditions, which has never been done at Mars, is enabling to land human payloads (~20 metric ton payloads) within 50 meters of a target**
  - **Low-L/D = blunt rigid heatshield surrounded by a Hypersonic Inflatable Aerodynamic Decelerator (HIAD)**
  - **Mid-L/D = slender rigid aeroshell with body flaps**

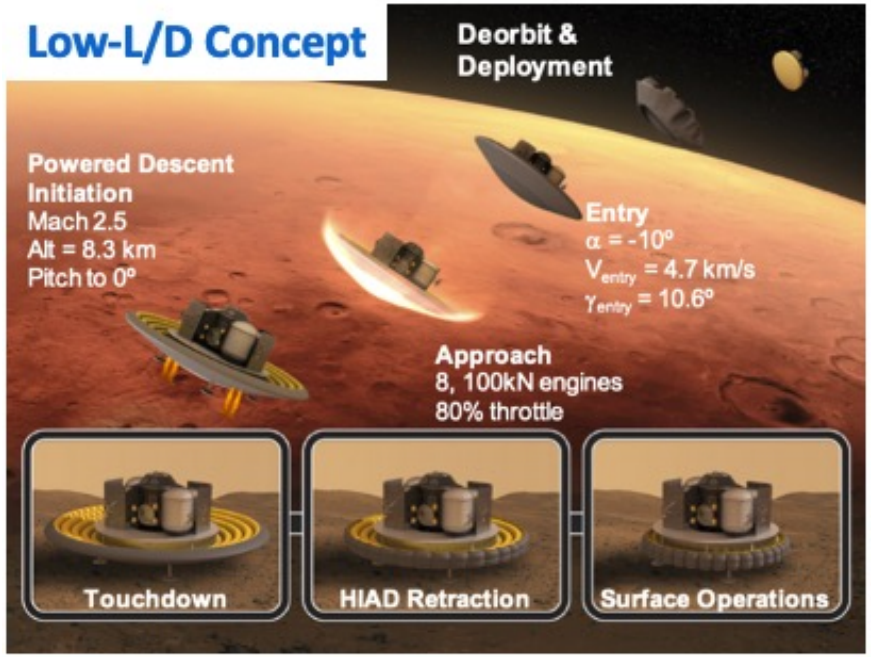

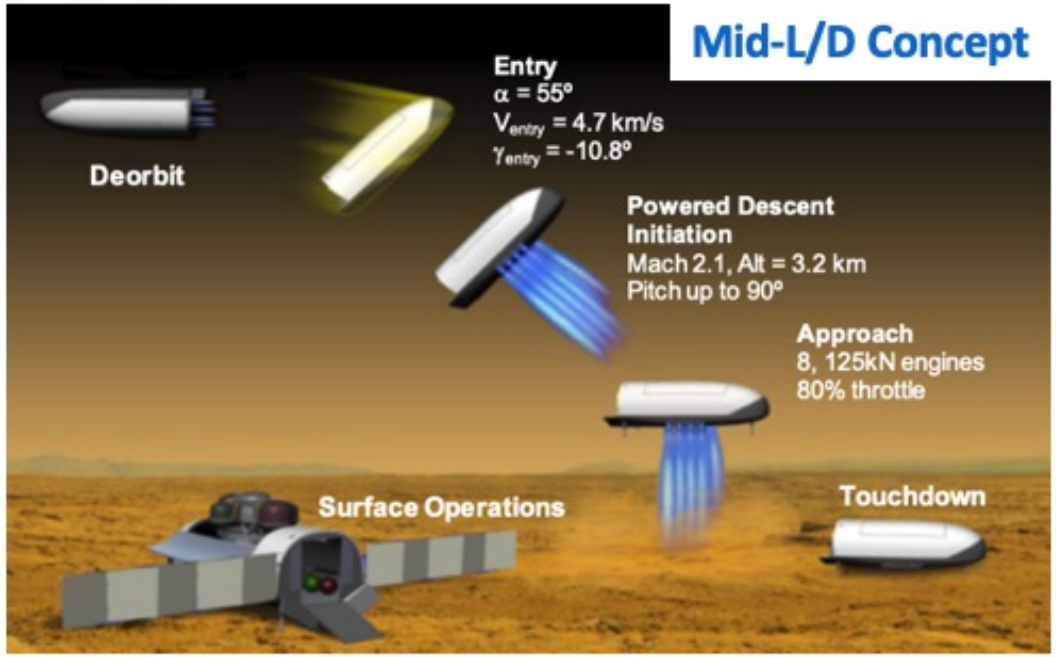

Edquist, et al, "Model Design and Pre-Test CFD Analysis for a Supersonic Retropropulsion Wind Tunnel Test," AIAA 2020-2230

- **Relevant ground test data do not yet exist to determine the computational fluid dynamic (CFD) predictive capabilities for vehicle aerodynamics during powered descent**

This presentation discusses the status of testing sub-scale Mars retropropulsion models in the Langley Unitary Plan Wind Tunnel (LUPWT) in 2022

Motivation

- **The most challenging aerosciences problem for large-scale Mars entry systems is aerodynamic interference (AI) during powered descent**
- **NASA's Aerosciences Evaluation and Test Capability (AETC) program established a project to determine whether CFD methods are sufficiently accurate for calculating "challenging" aerosciences problems at "high supersonic" conditions**
  - **Using the NASA Langley Unitary Plan Wind Tunnel (UPWT)**

This presentation discusses the status of an upcoming retropropulsion test in the Langley UPWT and pre-test CFD analysis of Mars retropropulsion concepts

- **Current status: The test had been planned to be completed as far back as late 2020, but COVID-19 and facility repair/maintenance delays have pushed the test to start no earlier than Sept. 2022**

Outline

- Reference Vehicles
- Test Facility
- Models & Instrumentation
- CFD Solvers & Sample Results
- Summary & Conclusions

- The wind tunnel test is funded by the Aerosciences Evaluation and Test Capabilities (AETC) office and the CFD is funded by the Space Technology Mission Directorate (STMD) Game Changing Development (GCD) program

- Presentation is adapted from AIAA Paper 2022-0911 and AIAA Paper 2022-0912

Flight Reference metric tons at entry)

Low-L/D

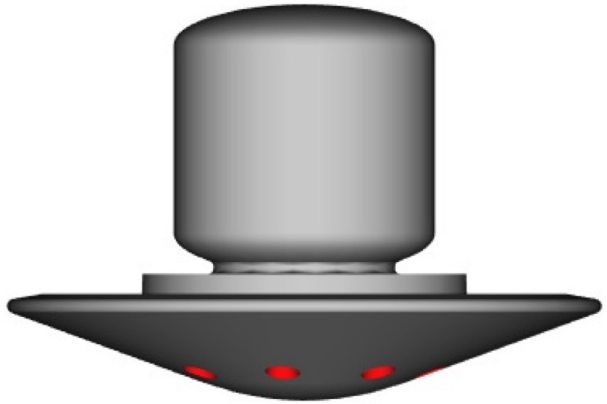

16.4 m

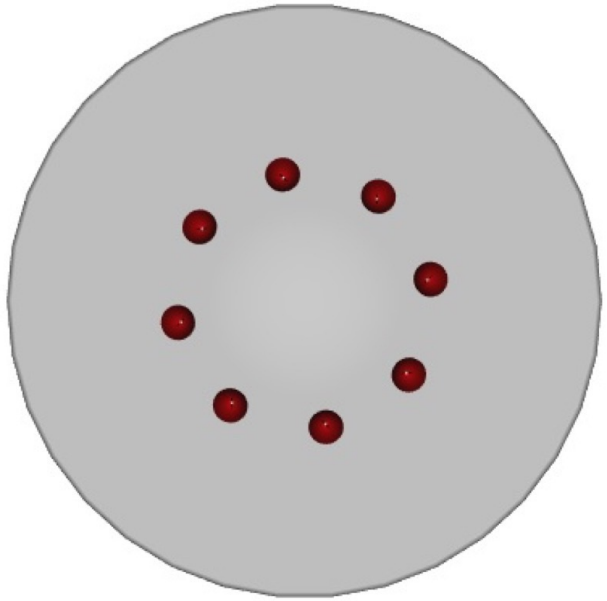

Mid-L/D

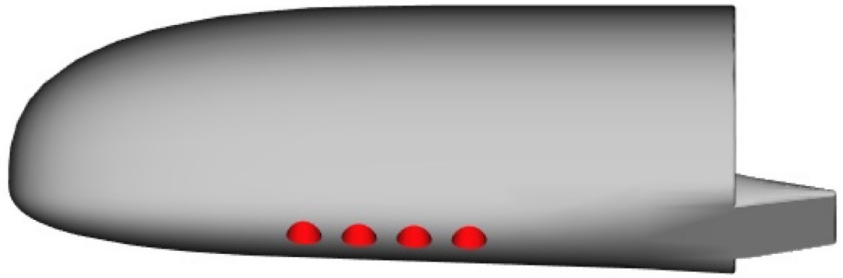

19.8 m

MSL & Mars 2020
~3 metric tons at entry
(to scale)

4.5 m

Nominal Reference Trajectories

- Eight LO_2/LCH_4 engines, 177:1 area ratio (AR = A_e/A^*) nozzles
  - 96 kN engines for Low-L/D (~50 tons at entry), 120 kN for Mid-L/D (~60 tons)

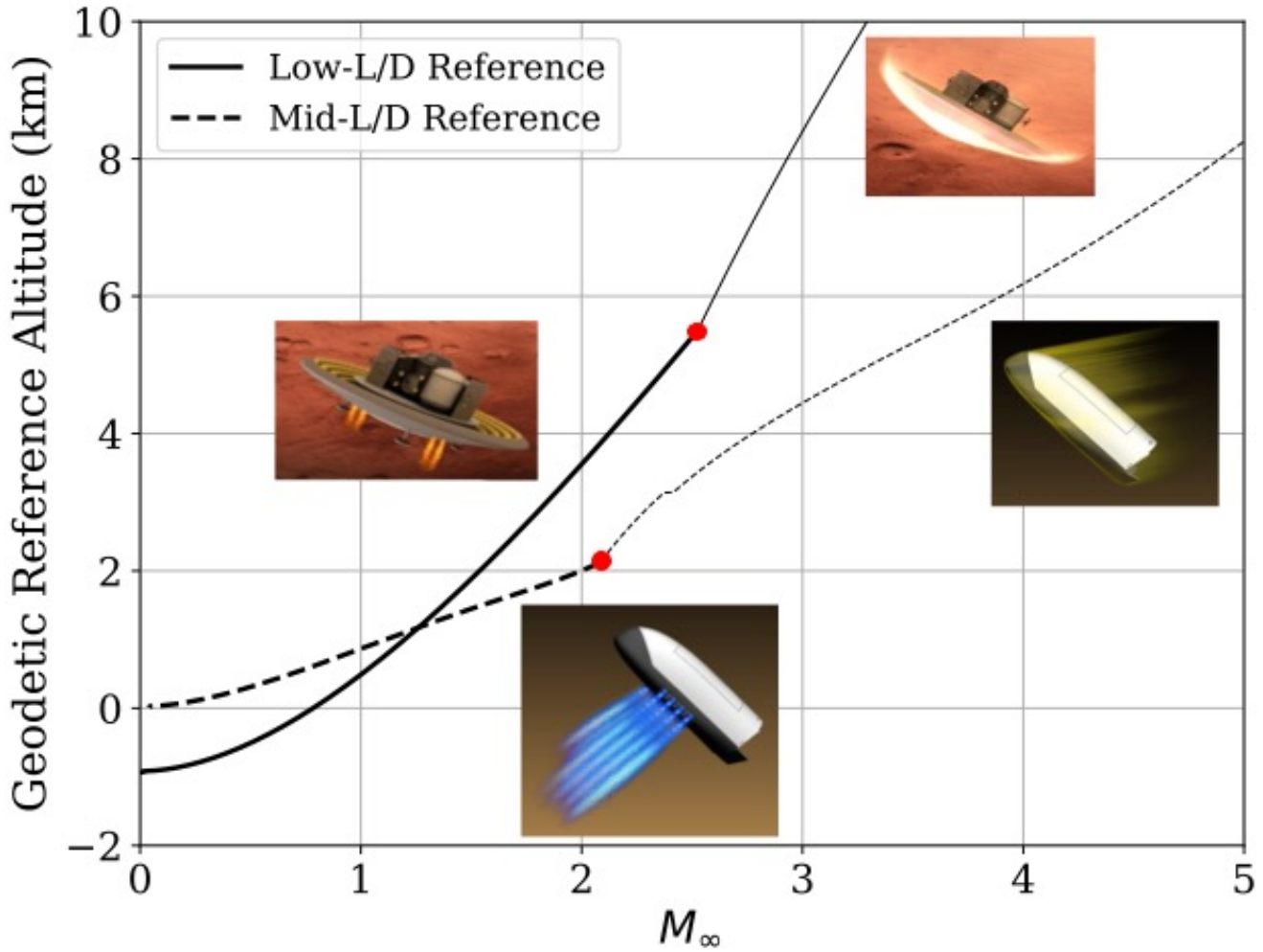

Wind Tunnel Test Objectives

1. **Design and fabricate subscale versions of the two Mars reference powered descent vehicles, to test in the LUPWT**
2. **Test the models over a range of Mach numbers, angles of attack, roll angles, nozzle configurations, and thrust levels that envelope the flight conditions as much as possible**
3. **Complete uncertainty quantification (UQ) analysis of the test data**
4. **Provide data for comparison to CFD results**

LUPWT Test Section 2

- **Mach number (2.30 to 4.63) is controlled with an asymmetric sliding-block nozzle, which is used to select the ratio of the nozzle throat area to test section area**
- **A re-characterization of test section 2 recently was completed to select conditions for the upcoming test**
  - **The rake data will also be factored into the test data UQ analysis**

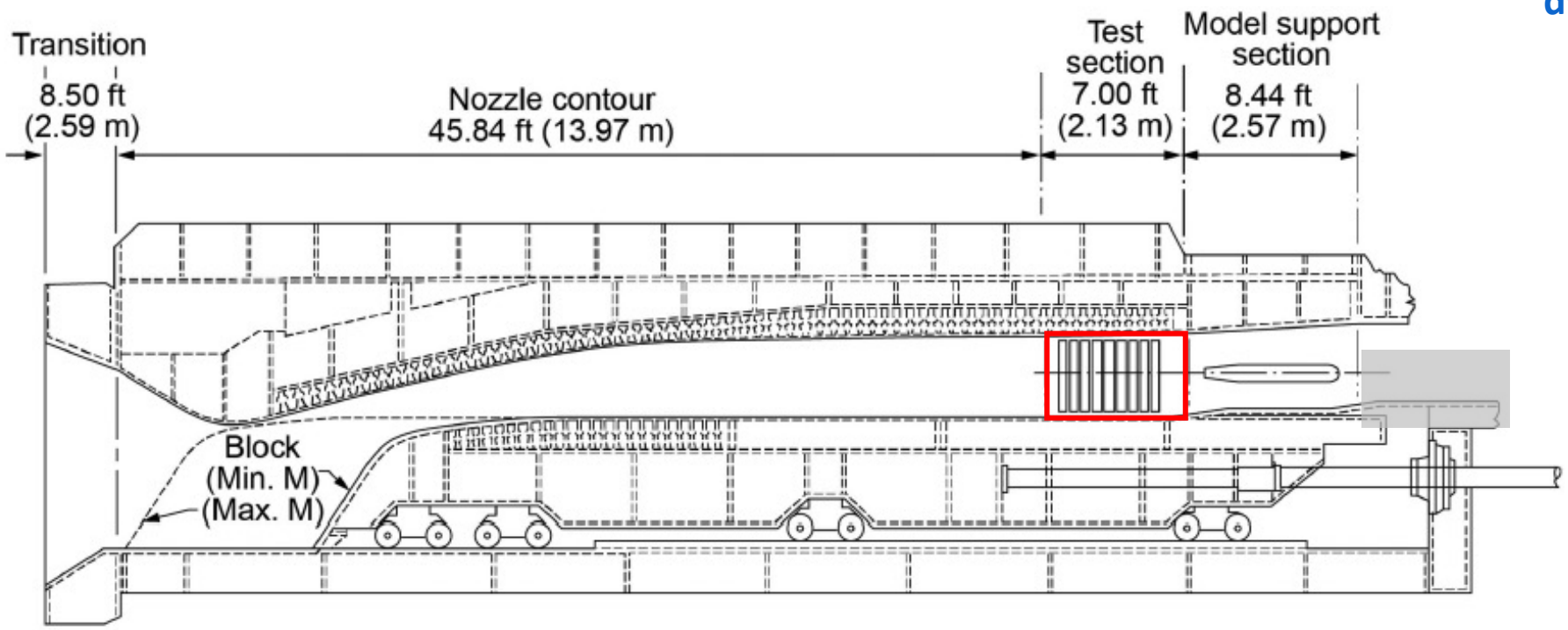

Probe rake used for test section re-calibration (Mach number, dynamic pressure, flow angularity)

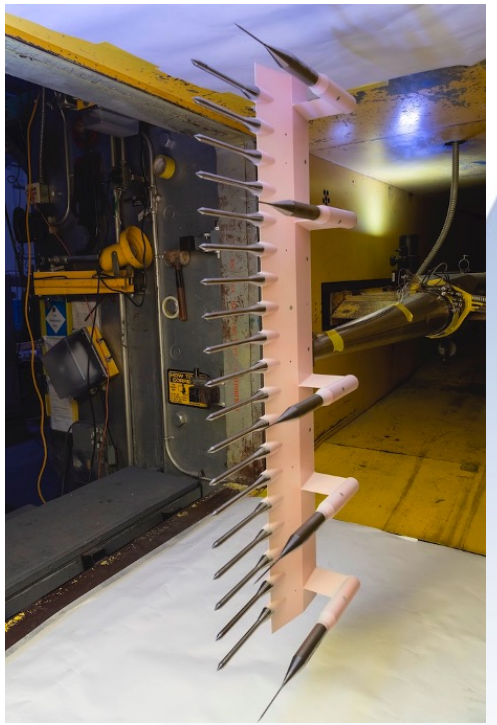

2010 Wind Tunnel Test

- **Objective: Provide SRP data for CFD validation**
- **Generic 5” dia. model with 0, 1, 3, 4 cold-gas air nozzles**
- **Mach = 2.6, 3.5, 4.6**
- **AoA = 0, ±4, ±8, 12, 16, 20**
- **Thrust Coefficients: CT = 0.5 to 4+**

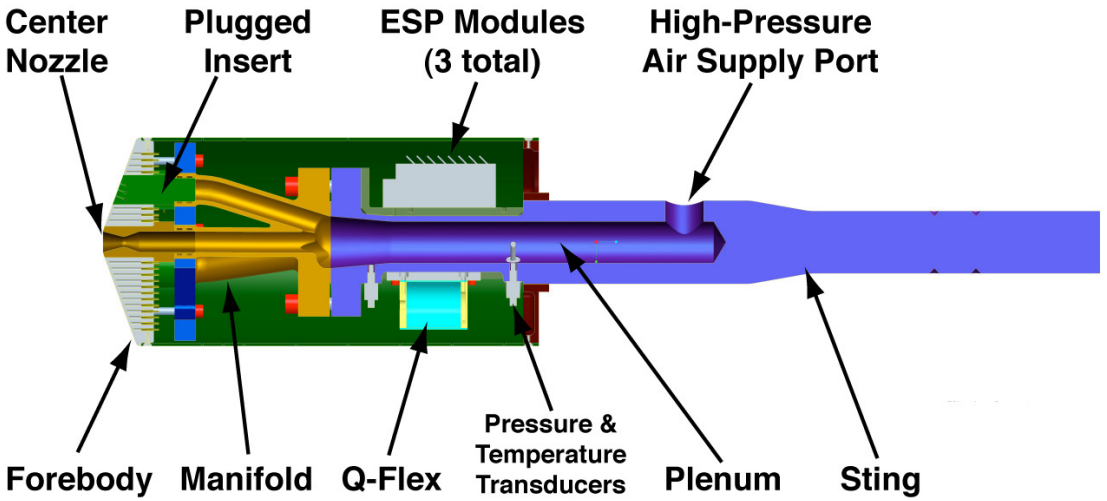

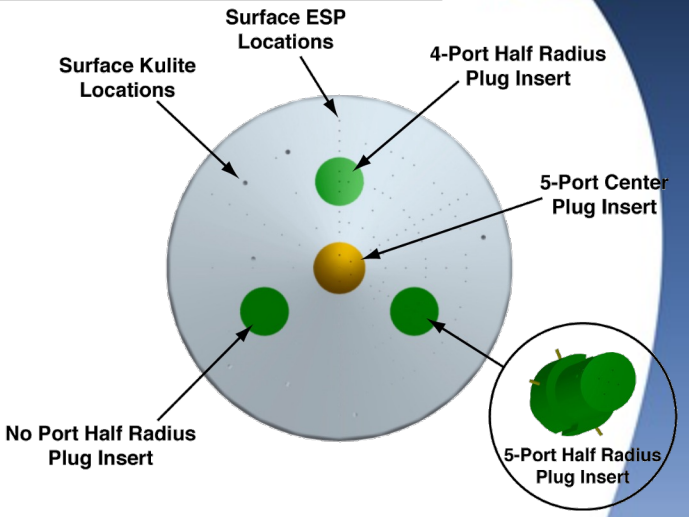

Pressure Instrumentation:

- **118 Forebody Surface (ESP)**
- **7 Forebody Surface (Kulites)**
- **49 Aftbody Surface (ESP)**
- **4 Internal (Kulites)**

2010 Wind Tunnel Test
Sample Schlieren Videos, Mach 4.6

- **Videos were captured at 6 to 10K frames per second**

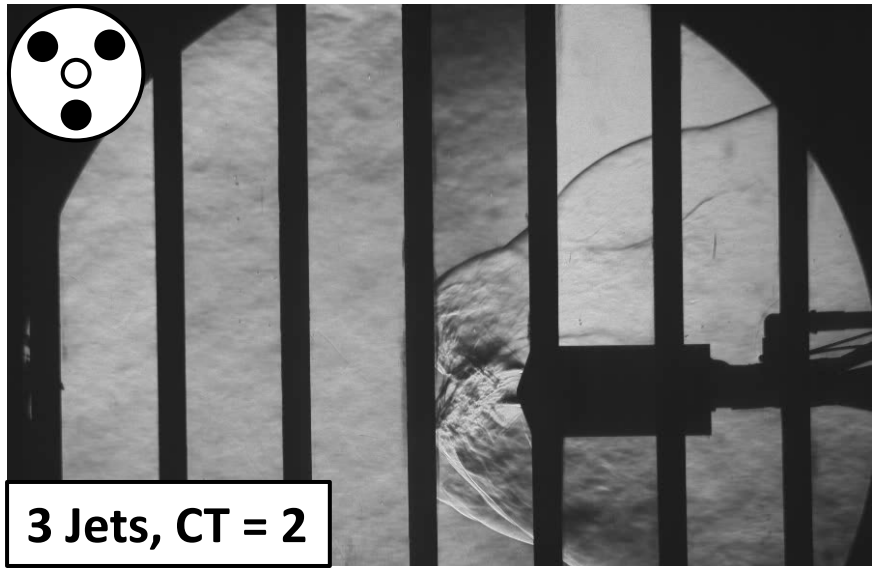

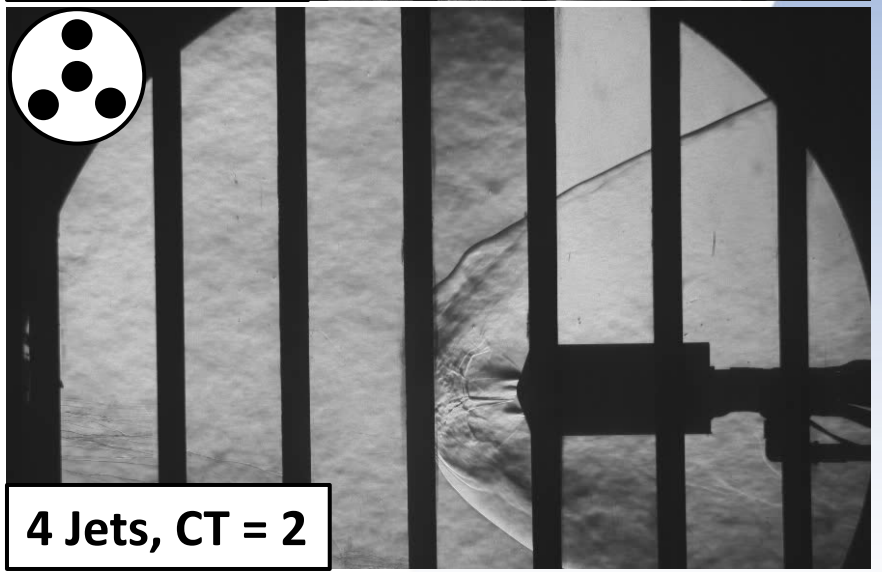

2010 Test, Effect of Thrust Coefficient
1 Jet, Mach = 2.4, AoA = 0

- **Higher thrust pushes out the bow shock and creates a larger jet barrel due to a higher degree of jet under-expansion**
  - **Full-scale vehicle CTs > 10 are needed based on EDL-SA studies**

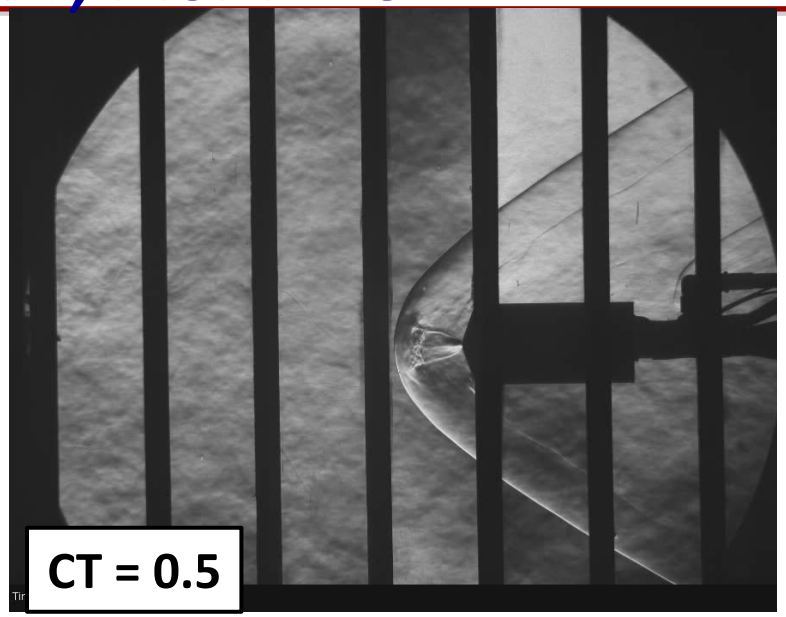

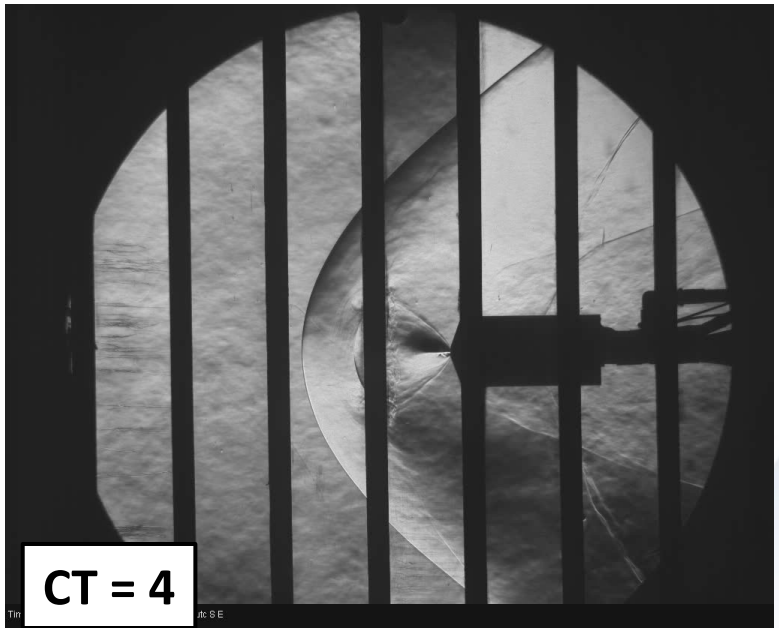

2010 Test, Comparison to CFD

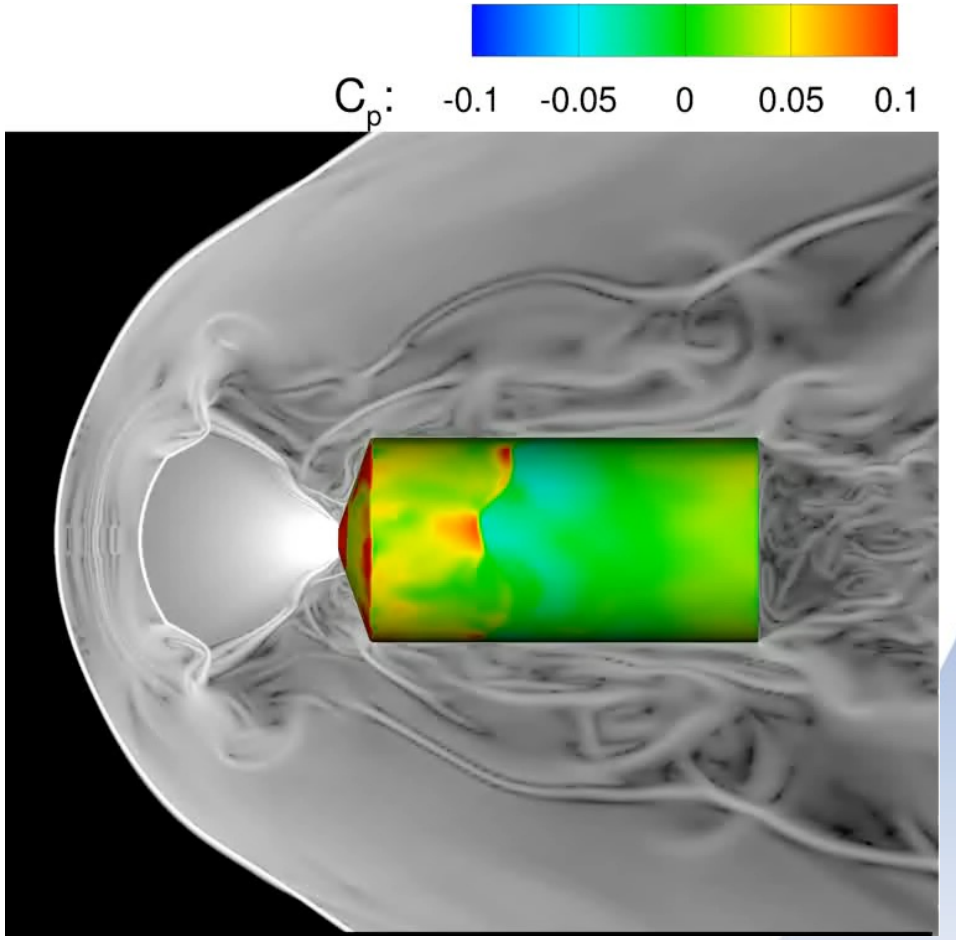

New Wind Tunnel Models

- High-pressure air (HPA) will flow through the model nozzles to simulate retrorockets
- The Low-L/D heatshield will have interchangeable nozzles that vary in size, location, cant angle, and area ratio

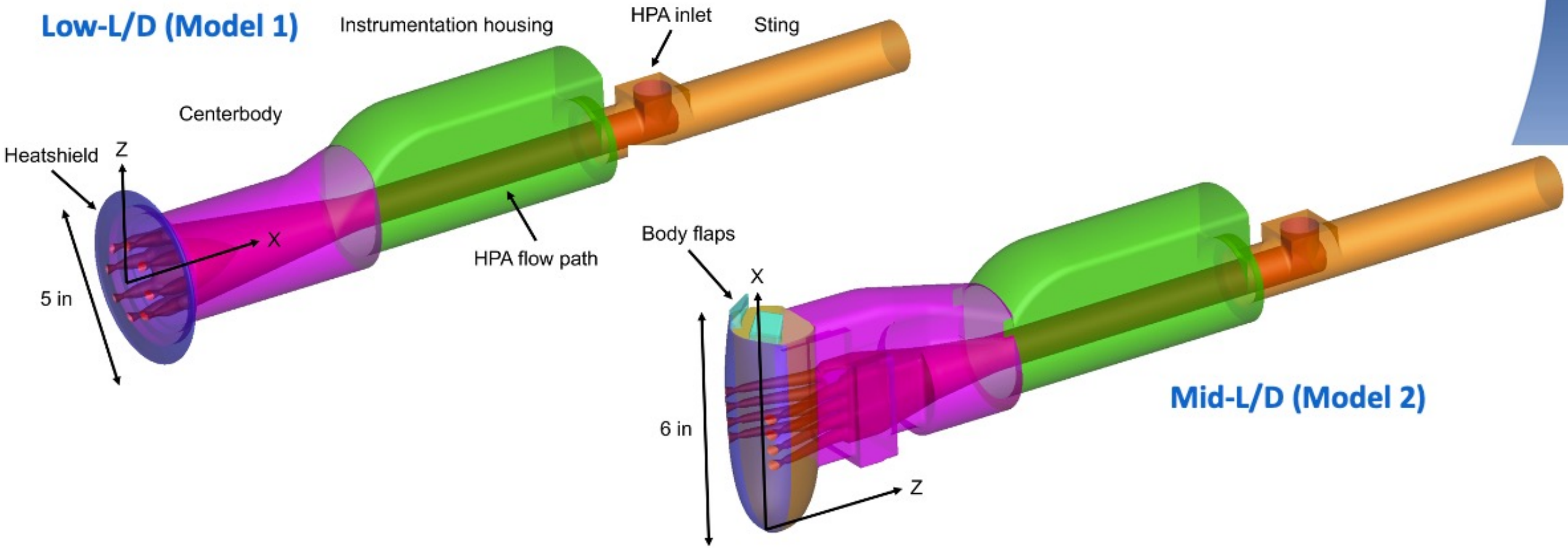

Wind Tunnel Model Scaling

- **Geometric scaling** is used for the model geometries, based on the reference vehicles
- **Jet scaling** is used to tailor the nozzle conditions to approximate the important jet interaction parameters that govern the aero/propulsive interaction flowfield, such as:
  - Thrust coefficient, C_T = Thrust / (1/2 $\rho_\infty V_\infty^2 S_{ref}$)
  - Ratio of nozzle exit pressure and stagnation pressure, $p_e / p_{0,2}$
- The wind tunnel models will use HPA to simulate the retro-rockets, so true scaling of the flight reference vehicles is not possible

Since HPA must be used for the nozzles instead of rocket engines, and because air and the combustion products differ thermodynamically, only one jet scaling parameter at a time can be matched to flight

Low-L/D Nozzle Variations

- **The Low-L/D heatshield has interchangeable nozzles that are expected to impact test results:**
  - **Exit area relative to heatshield area**
  - **Radial distance from nose (R_n/R_b)**
  - **Cant angle (θ_{cant})**
  - **Exit-to-throat area ratio (AR), limited by using unheated HPA (T_0 = ~250 deg. F)**
  - **Spacing (evenly or paired)**

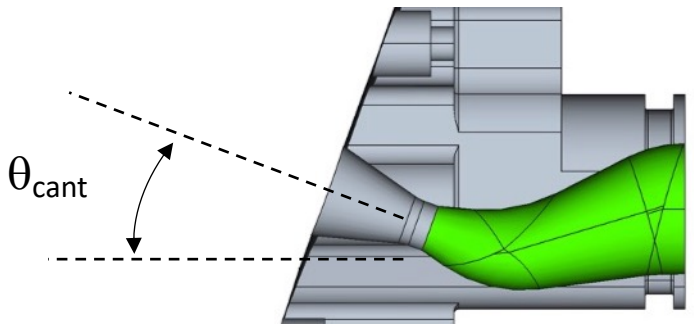

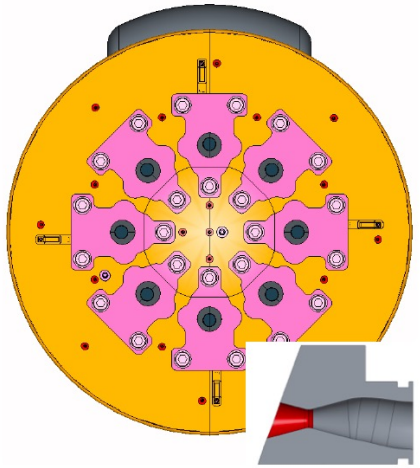

(a) 1A (AR=4, θ_{cant}=0°, R_n/R_b=0.434)

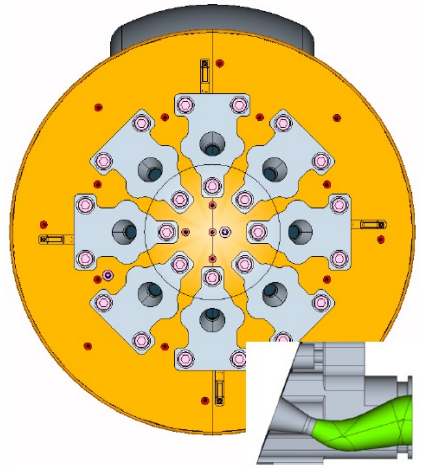

(b) 1B (AR=4, θ_{cant}=20°, R_n/R_b=0.434)

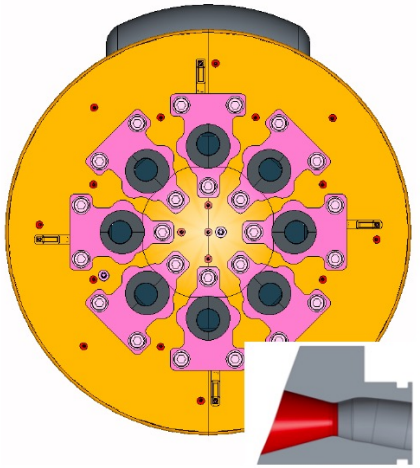

(c) 1C (AR=4, θ_{cant}=0°, R_n/R_b=0.434)

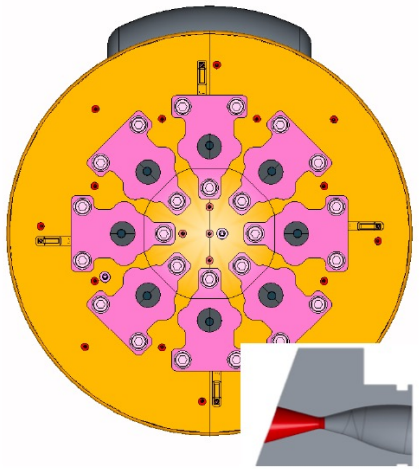

(d) 1D (AR=11, θ_{cant}=0°, R_n/R_b=0.434)

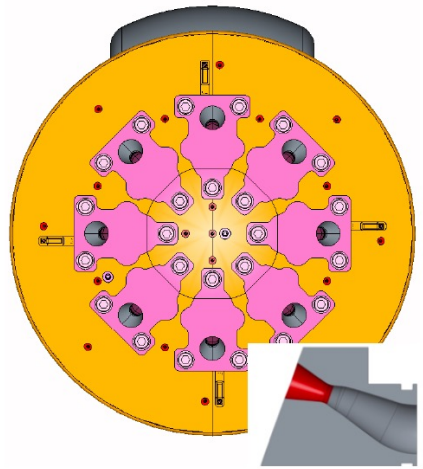

(e) 1E (AR=4, θ_{cant}=20°, R_n/R_b=0.6)

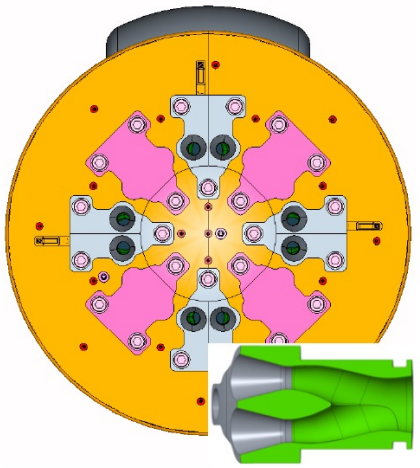

(f) 1F (AR=4, θ_{cant}=5°, R_n/R_b=0.434)

Low-L/D Model Hardware

- **Both models were inspected at NASA Langley in August 2020**

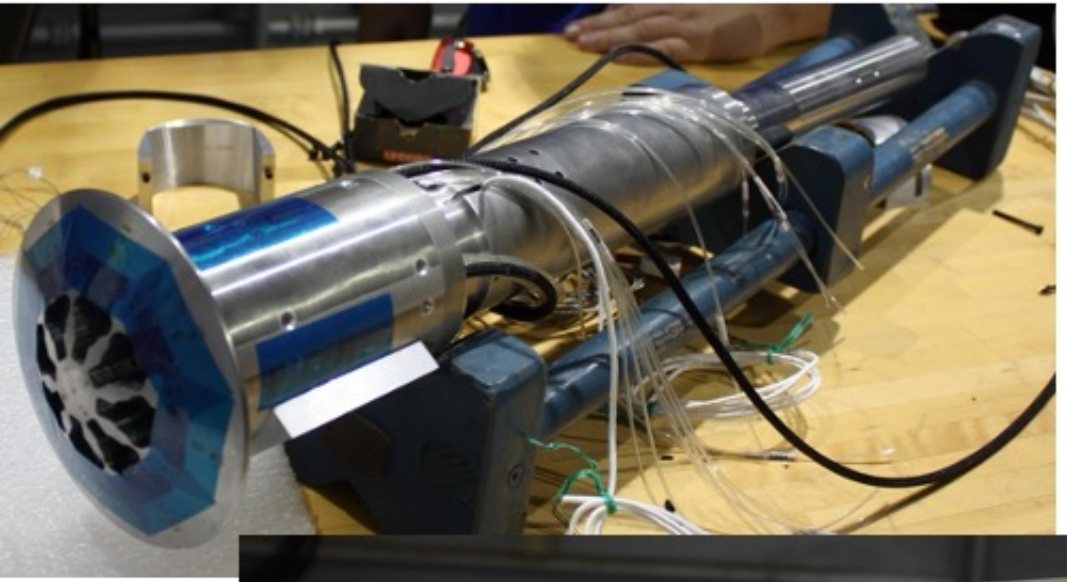

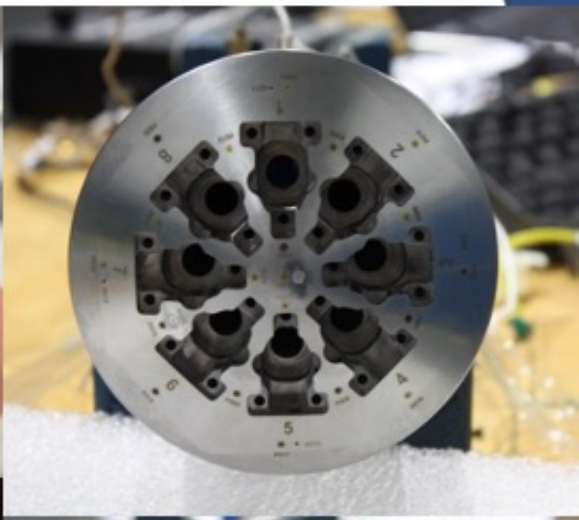

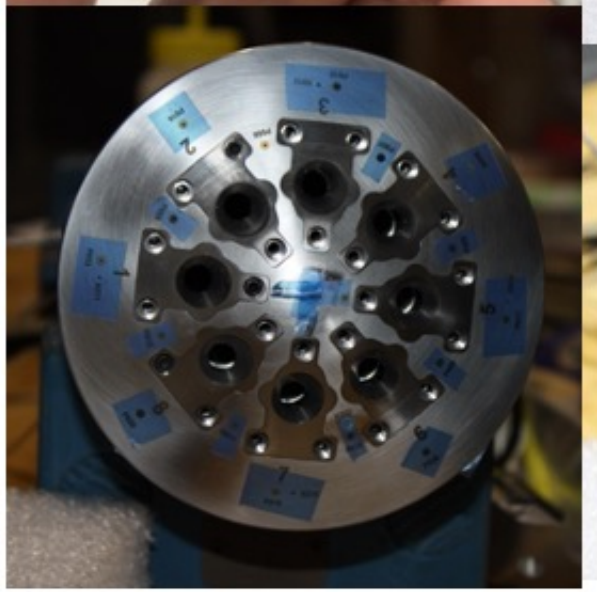

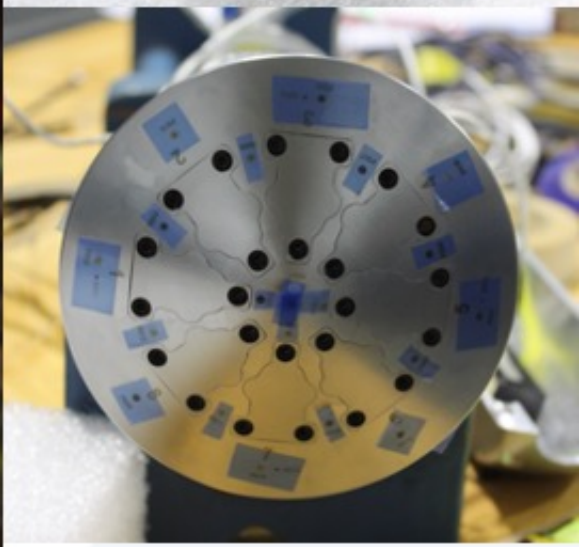

Mid-L/D Model Hardware

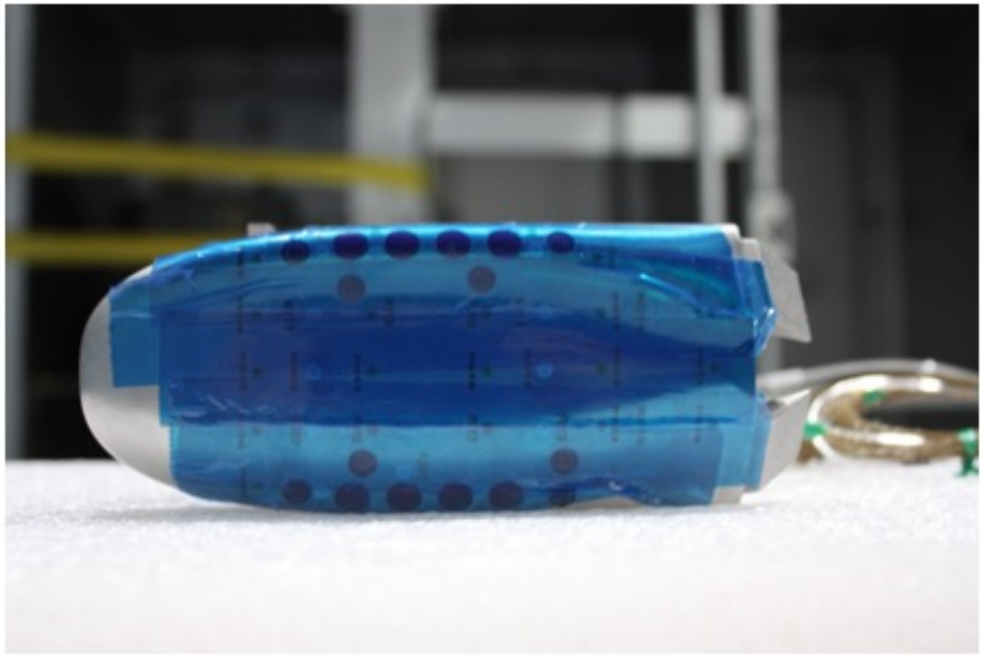

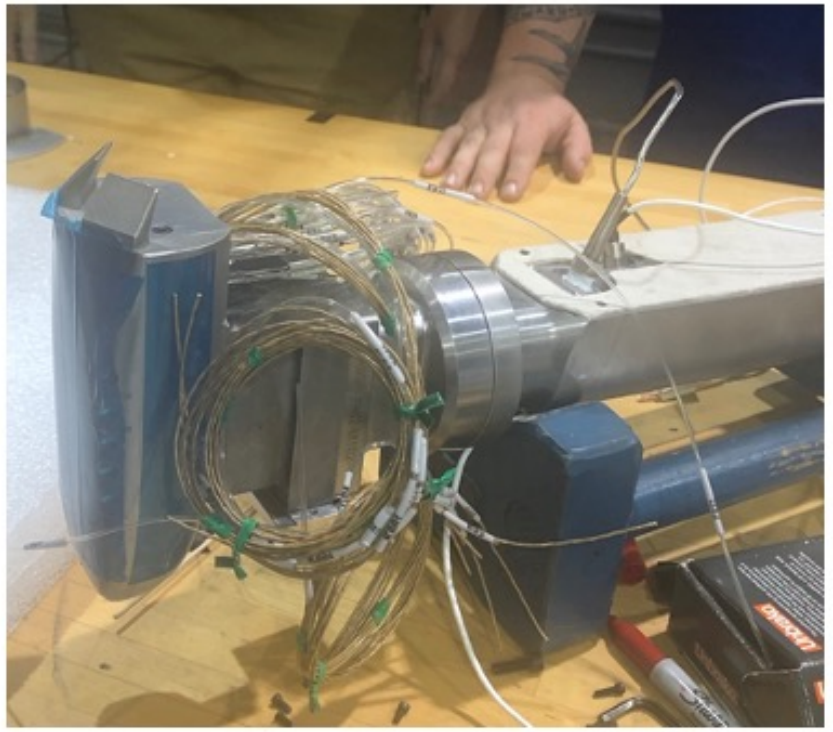

Instrumentation

- **Flow-through six-component force & moment balance (Burns, et al)**
  - **Added after model design & fabrication**
  - **Will be first known such retropropulsion measurements**
- **Discrete pressure (steady and unsteady) on heatshield**
- **Pressure-sensitive paint (PSP) on heatshield**
- **High-speed schlieren video (~10 kHz)**
- **Oil-based nozzle plume seeding for flow visualization (Acharya, et al)**
  - **Added after model design & fabrication**
- **HPA total pressure and temperature**

Balance design

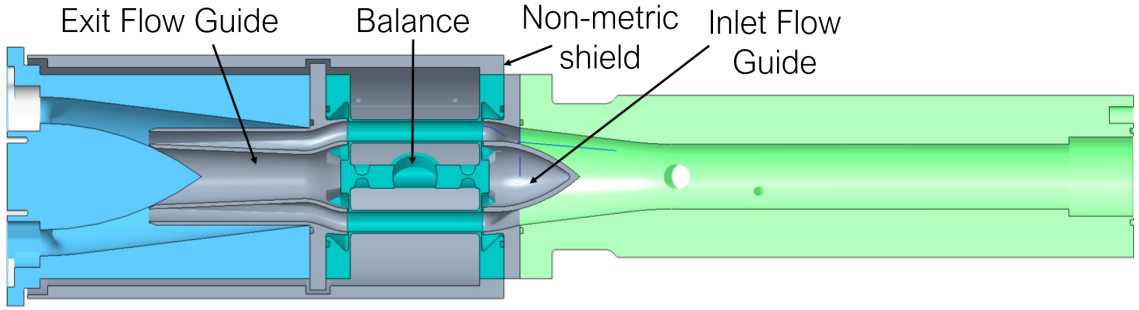

HPA measurements

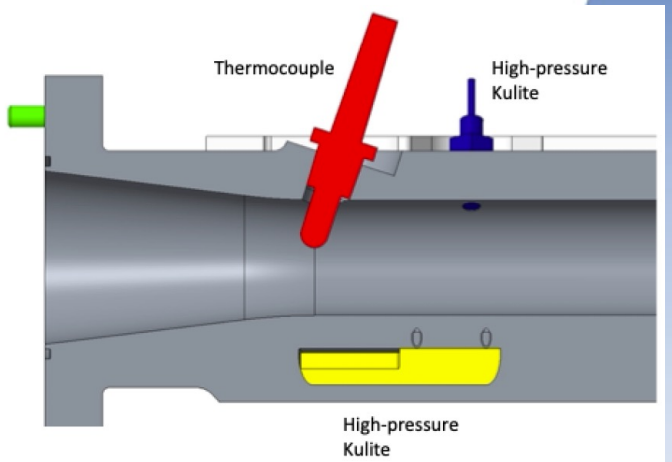

Heatshield pressure

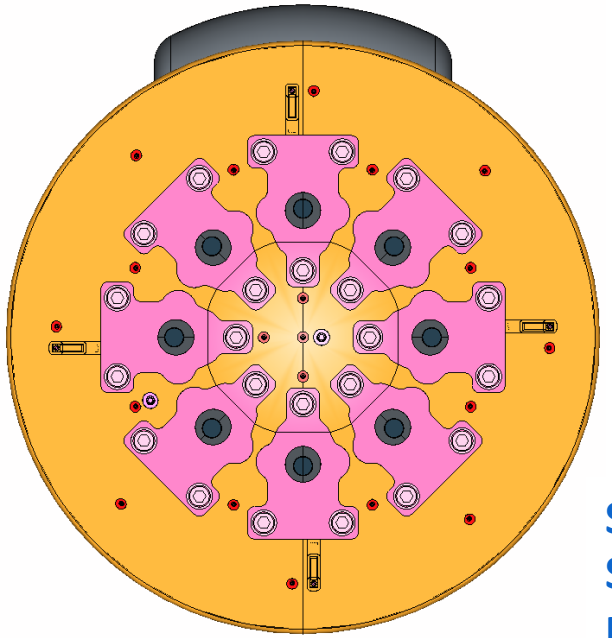

Surface covered in PSP
Steady pressure
High-frequency pressure

Test Matrix Parameters

- **The number of different values for some parameters will be determined by how much time it takes to make model/tunnel changes and by which measurements are being made, not all of which can be done at the same time**

	Low-L/D Model	Mid-L/D Model
Nozzle configurations	1 (plugged), 1A, 1B, 1C, 1D, 1E, 1F,	2 (plugged), 2A
M_∞ and Re_∞/ft	2.4 and 1E6, 3.5 and 1E6, 4.6 and 1.5E6	
HPA total pressure	up to 1500 psia	
HPA total temperature	up to ~250 deg. F	
Angle of attack	-10 to 20 deg	70 to 100 deg
Roll angle	0 and 22.5 or 45 deg	0

Example Test Conditions for Model 1A

- Each model will be tested at combinations of Mach number (2.4, 3.5, 4.6), angle of attack, roll angle, and HPA total pressure (p_c)
- At each condition, p_c will be adjusted to achieve certain vacuum thrust coefficients (C_T) that envelope the nominal reference flight conditions

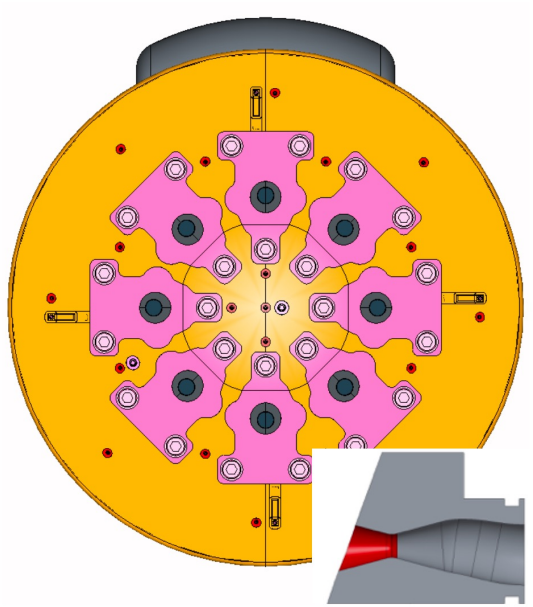

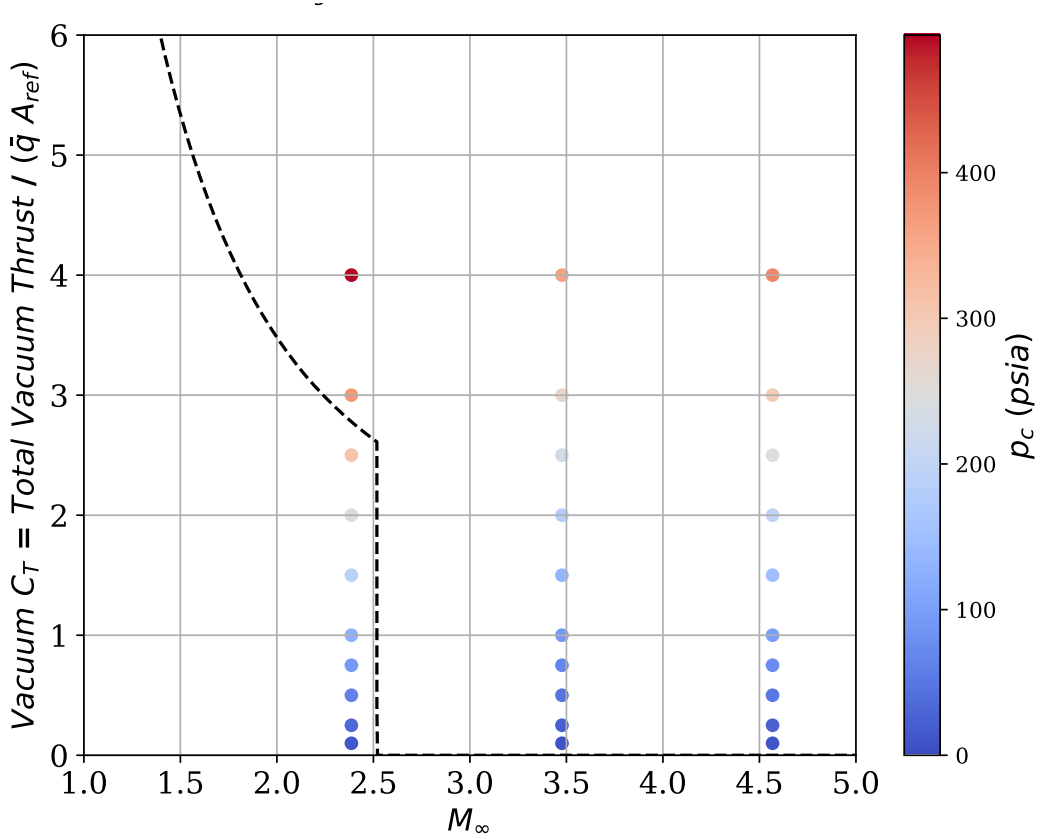

C_T = Thrust / ($1/2\rho V^2 S_{ref}$)

CFD Solvers

- **Loci-CHEM (F. Canabal)**
  - Finite volume, unstructured grids, ~200M grid cells
  - Cases to date have been run as unsteady Reynolds-Averaged Navier-Stokes (URANS)
- **OVERFLOW (R. Childs, L. Halstrom, K. Matsuno)**
  - Finite difference, overset structured grids with automatic mesh refinement (AMR), ~150-250M grid points
  - Cases to date have been run as URANS, will also run Detached Eddy Simulations (DES)
- **FUN3D (C. Glass, A. Korzun, W. Wood)**
  - Finite volume, unstructured grids with mesh refinement, ~50M grid points
  - Cases to date have been run as DES

Used in conjunction with retropropulsion wind tunnel testing in 2010/2011

- **Goal prior to test: solutions from at least 2 solvers per condition: 2 non-blowing + 7 blowing models, 3 Mach numbers, 3 thrust coefficients, 3 angles of attack**
- **More than 350 solutions completed to date**

CFD Boundary Conditions

- Tunnel inflow is taken from separate CFD solutions of the tunnel ahead of the test section – non-uniform, vortices at the wall corners, non-zero flow angularity
- Nozzle inflow is applied at total pressure and temperature on the plenum face

Tunnel Boundary Conditions

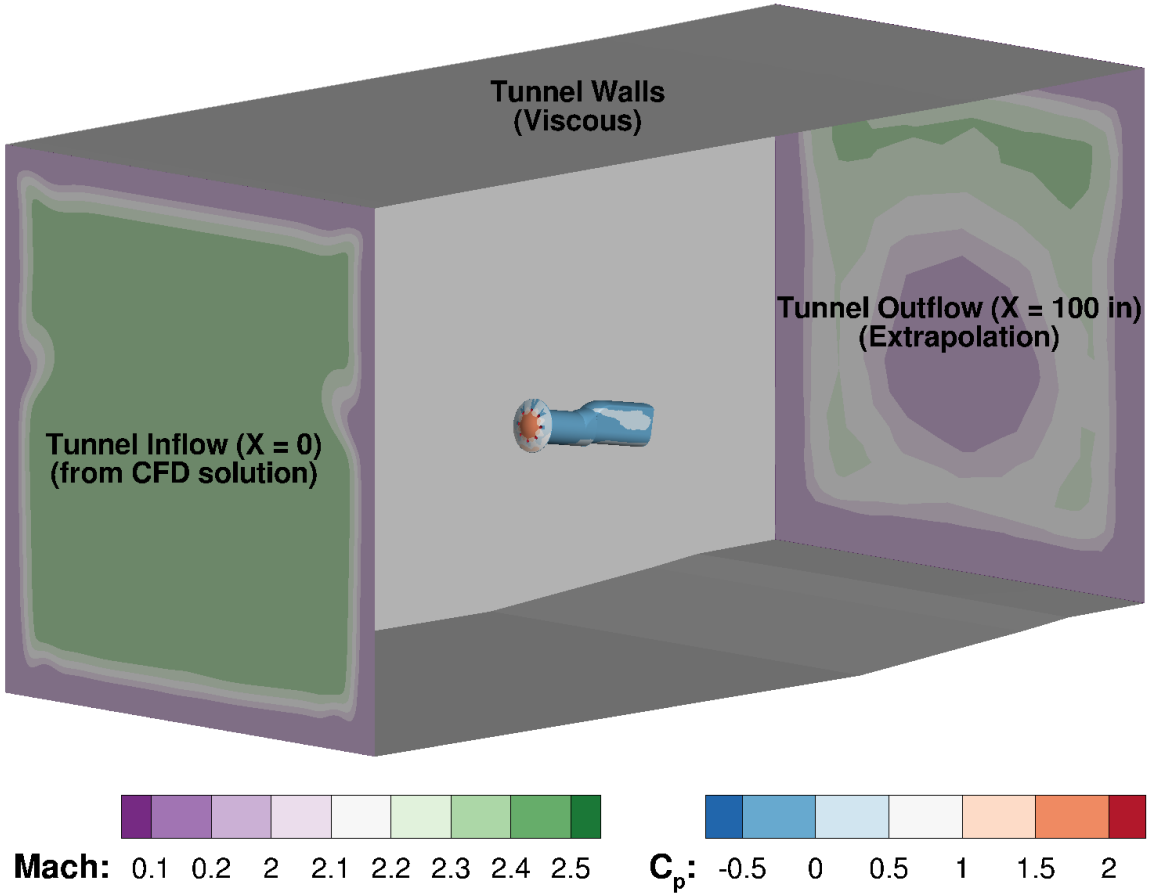

Model Boundary Conditions

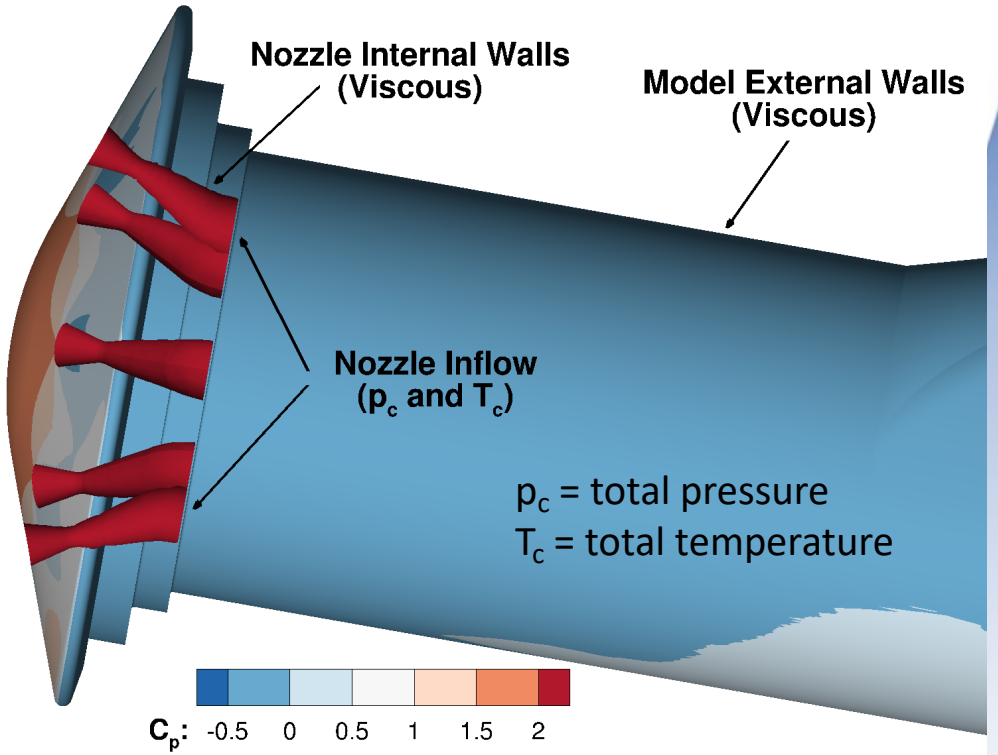

Sample Solution, Model 1A

- Tunnel Mach number = 2.4, model thrust coefficient (C_T) = 1, angle of attack = 10 deg
- Over 350 solutions have been completed to date with three solvers

FUN3D time-averaged Mach number and model surface pressure coefficient on adapted grid

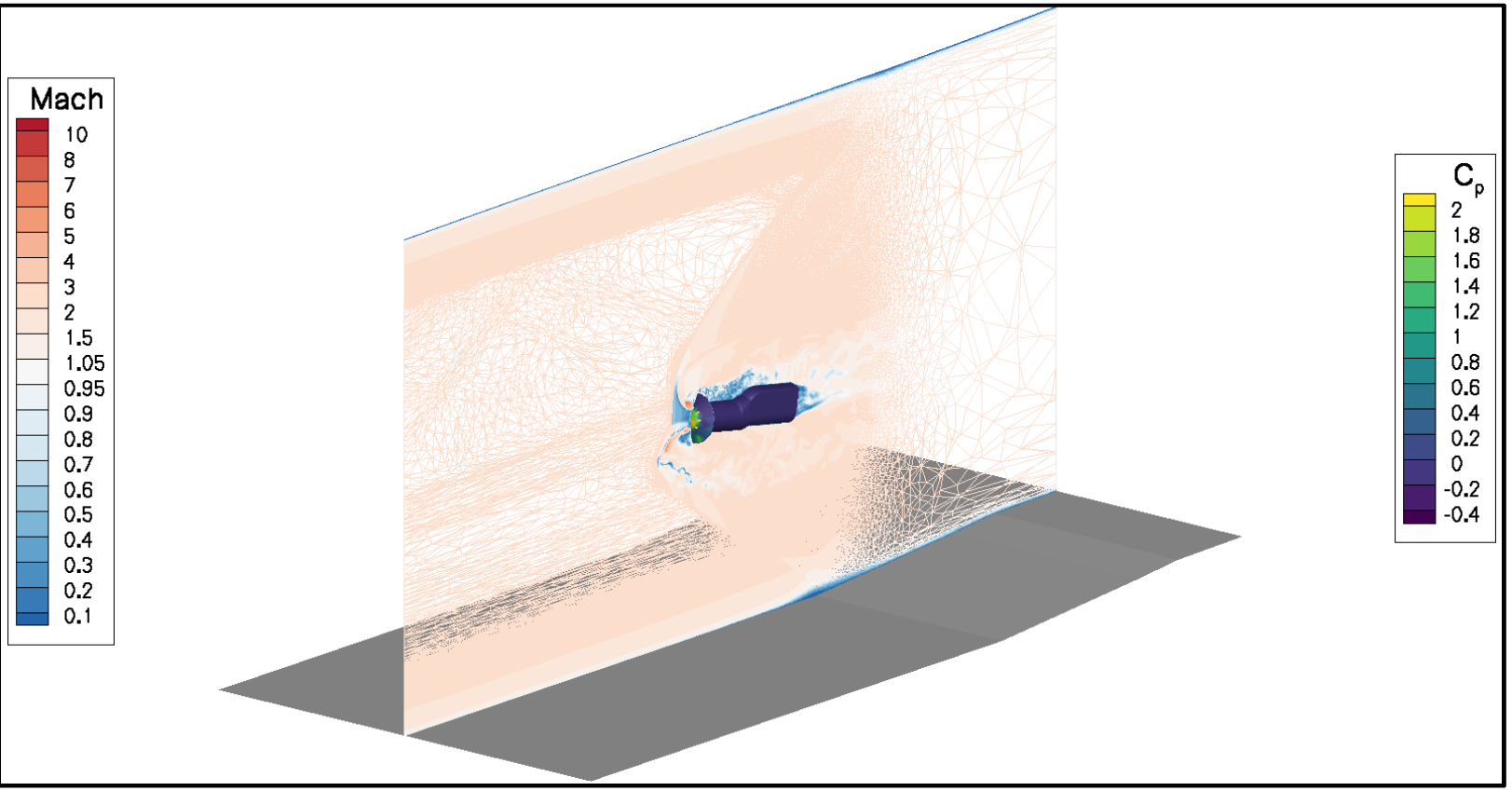

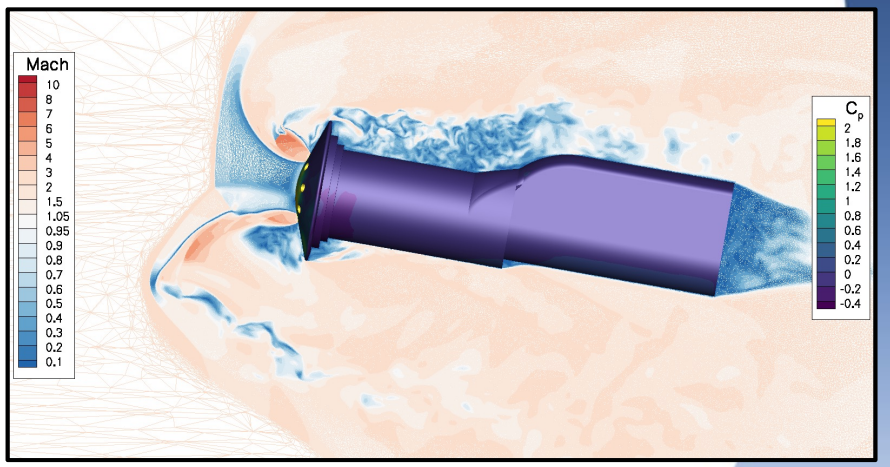

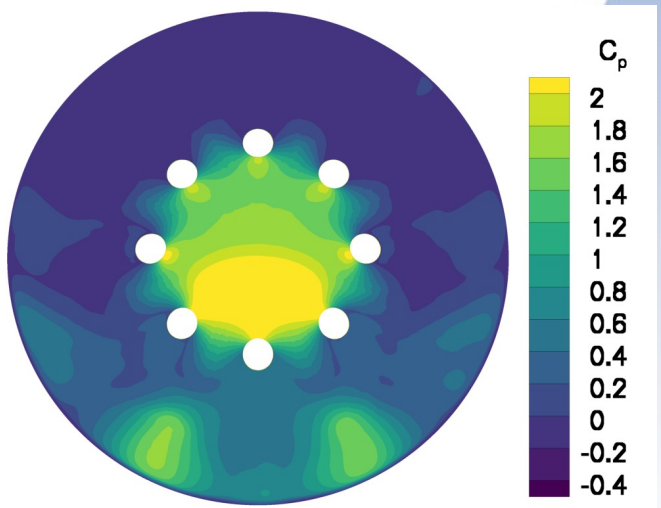

Predicted Effect of Thrust
Model 1A

- **Tunnel Mach number = 2.4, thrust coefficients (C_T) of 0, 0.5, 1, and 2.5**

C_T = Thrust / ($1/2\rho V^2 S_{ref}$)
AoA = angle of attack
$C_{F,x}$ = aerodynamic axial force coefficient

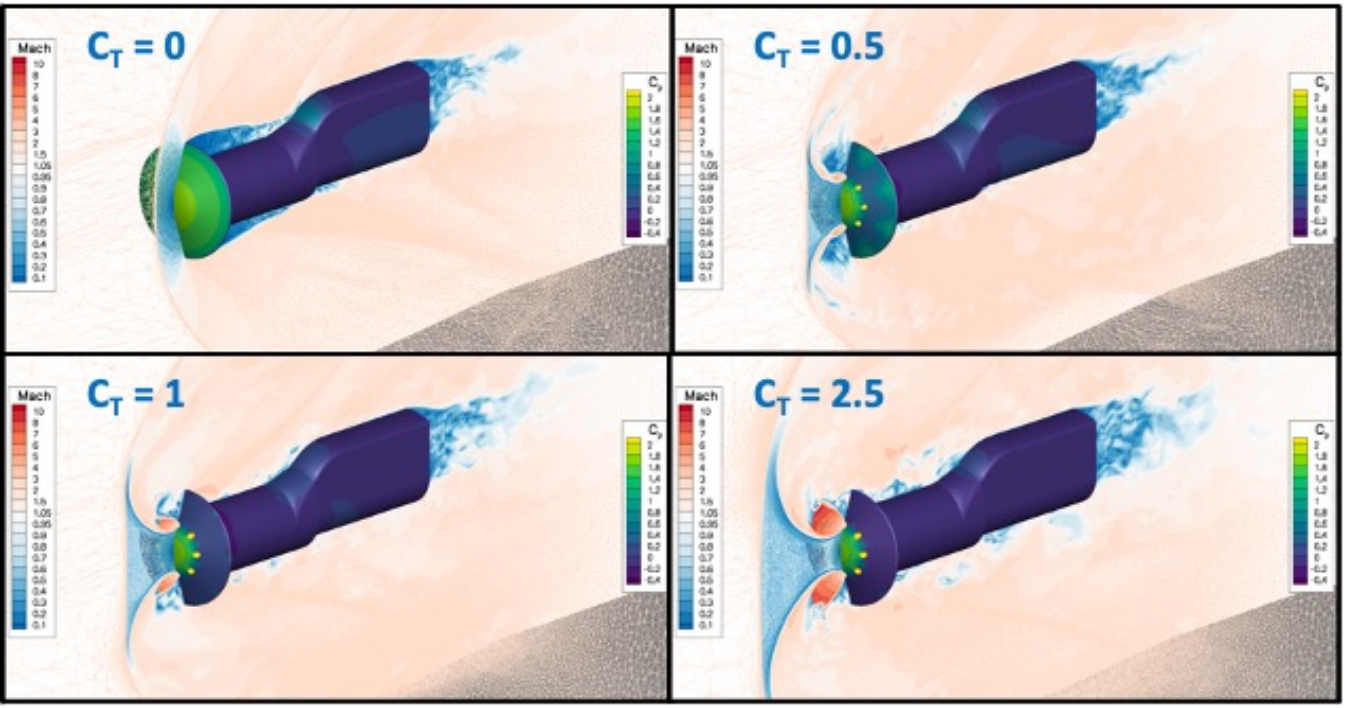

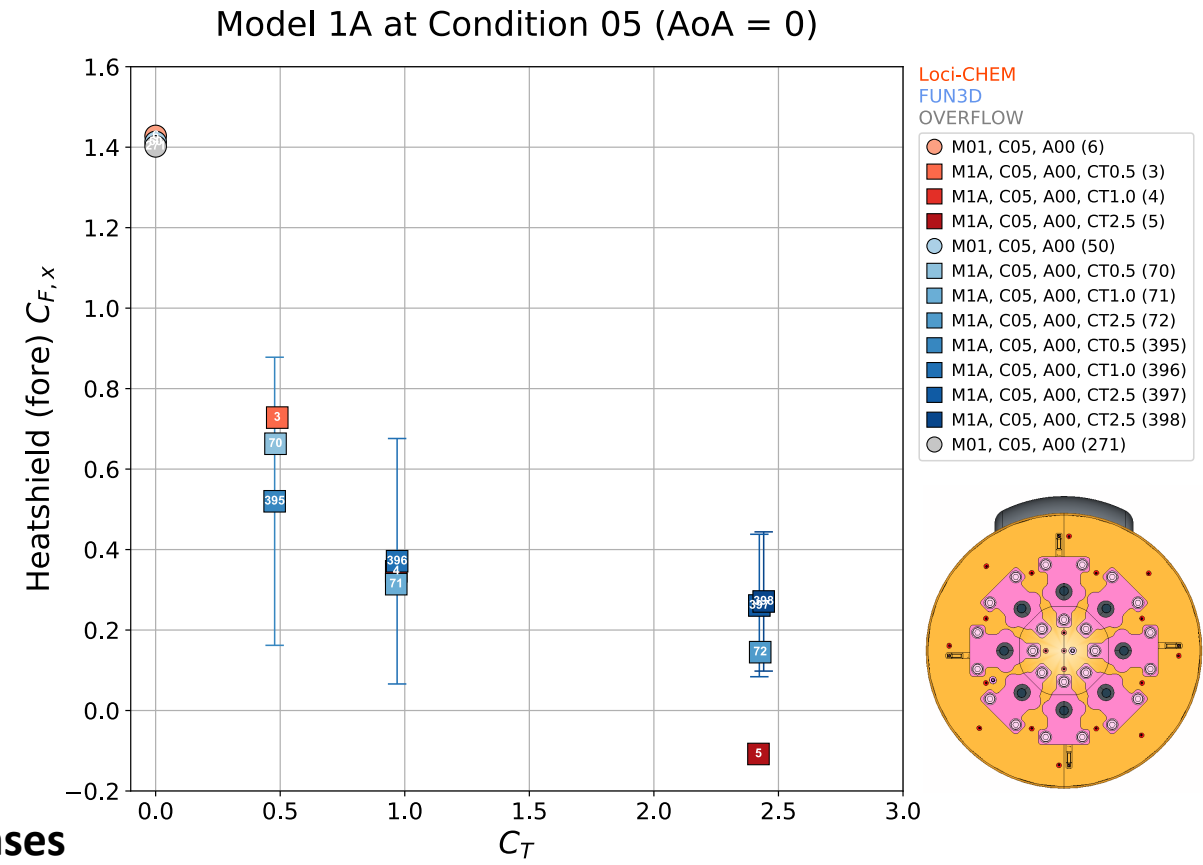

- **With increasing thrust:**
  - **Shock standoff distance increases**
  - **Heatshield aerodynamic axial force coefficient ($C_{F,x}$) decreases**
- **Significant scatter between CFD solvers, possibly due to URANS vs. DES, causes will be investigated further**

Predicted Effect of Thrust
Model 2A

- Tunnel Mach number = 2.4, thrust coefficients (C_T) of 0, 0.5, 1, and 2.5

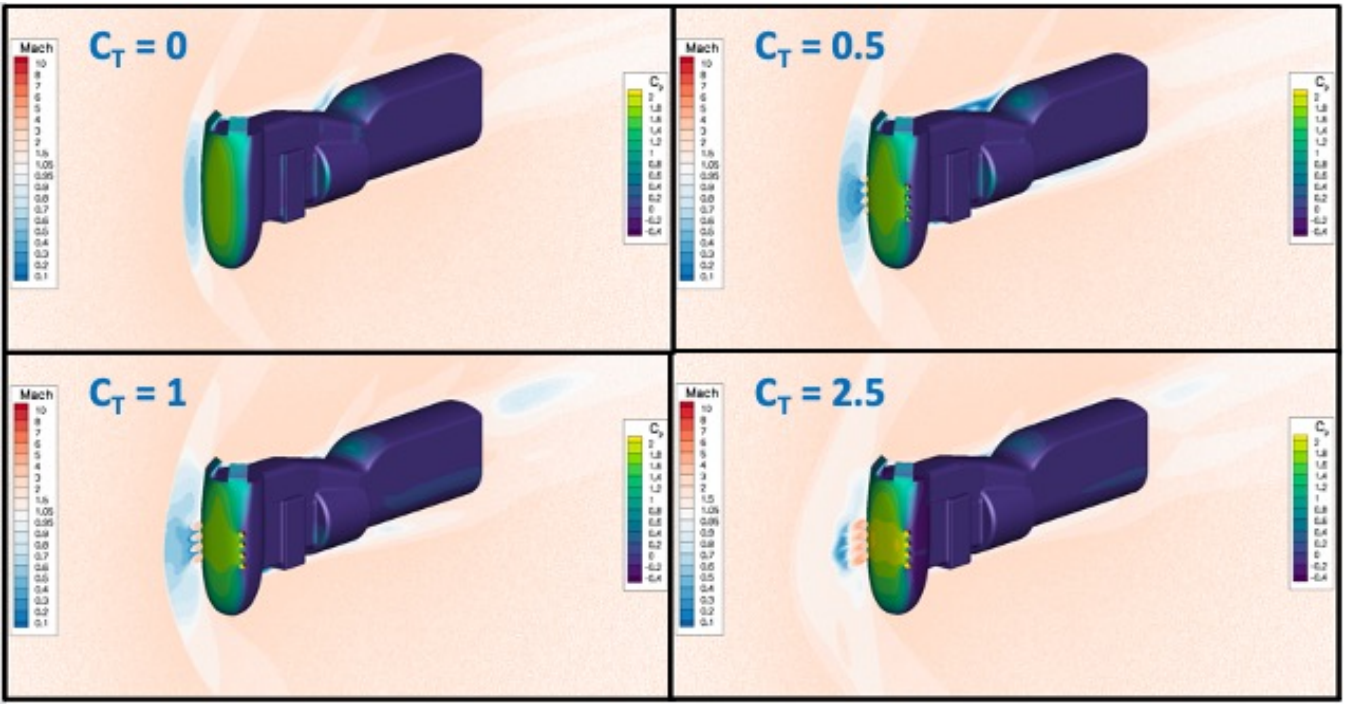

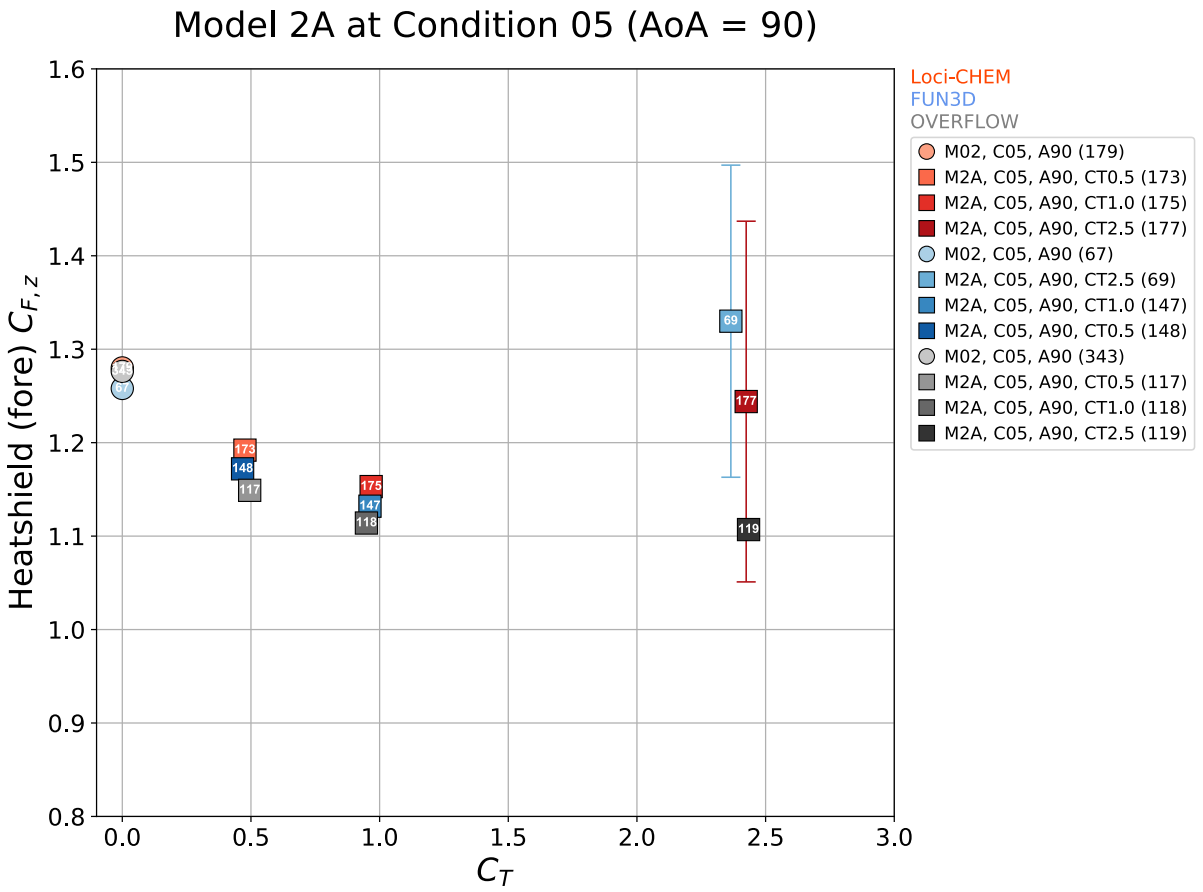

- With increasing thrust:
  - Shock standoff distance increases
  - Heatshield $C_{F,z}$ does not not monotonically decrease
- Significant scatter between CFD solvers at highest C_T

Predicted Effect of Nozzle Cant Angle Models 1A and 1B

- **If nozzles have an outward radial component (cant angle = 20-deg) for a given C_T:**
  - **Heatshield aerodynamic axial force coefficient increases due to reduced plume blockage inboard of nozzles**

Model 1A at Condition 05 (AoA = 0)

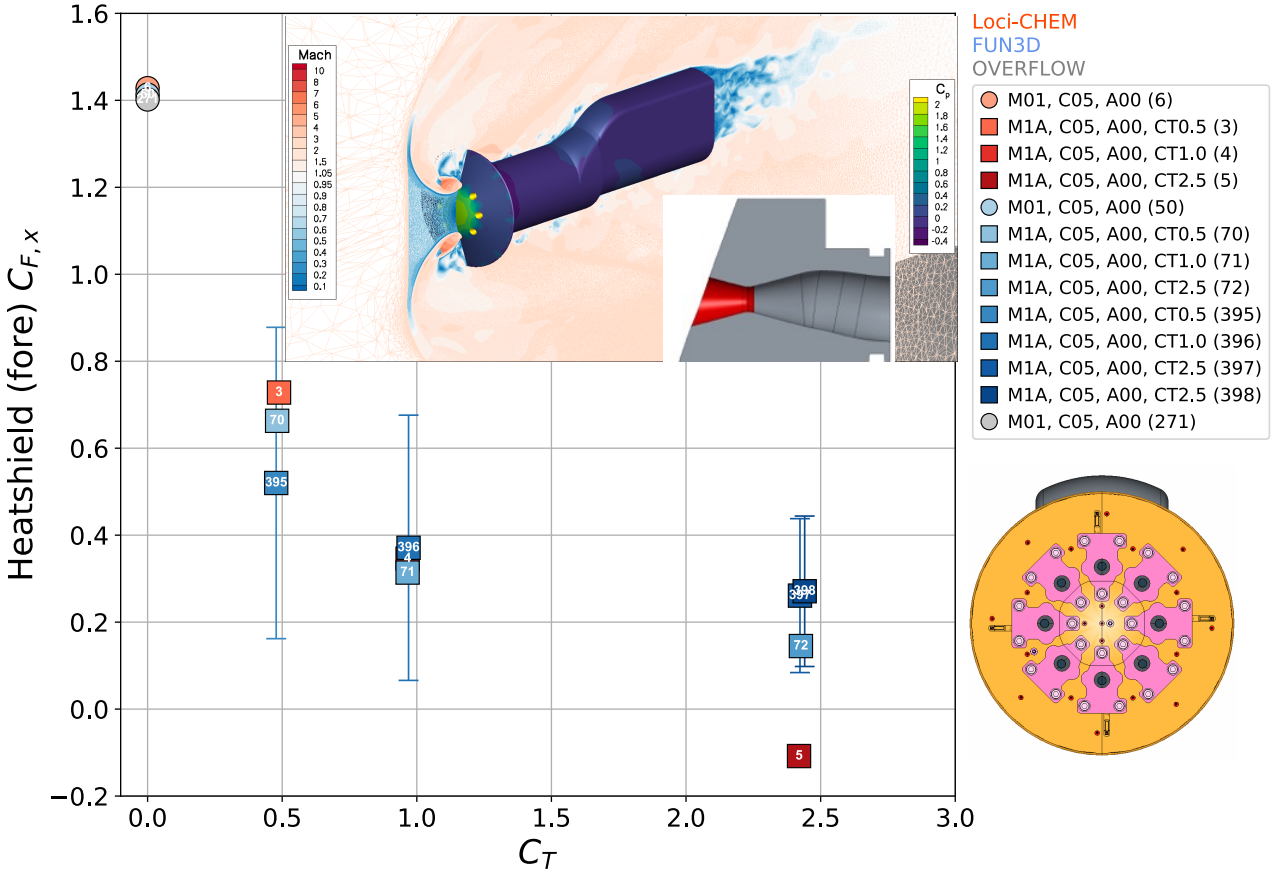

Model 1B at Condition 05 (AoA = 0)

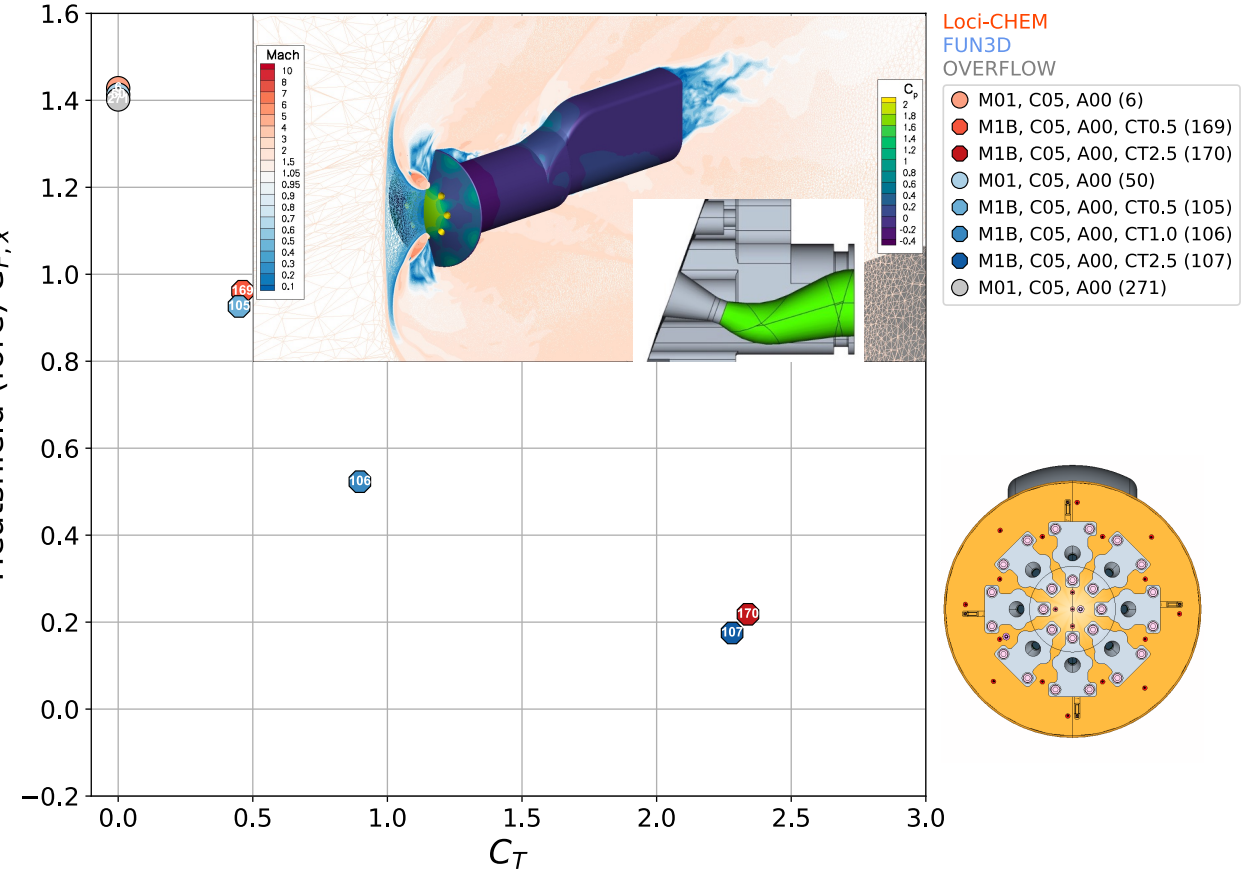

Predicted Effect of Nozzle Radial Location Models 1B and 1E

- **If nozzles are placed closer to the heatshield shoulder (model 1E) for $C_T > 0.5$:**
  - **Heatshield aerodynamic axial force coefficient increases due to larger area of high pressure inboard of nozzles**

Model 1B at Condition 05 (AoA = 0)

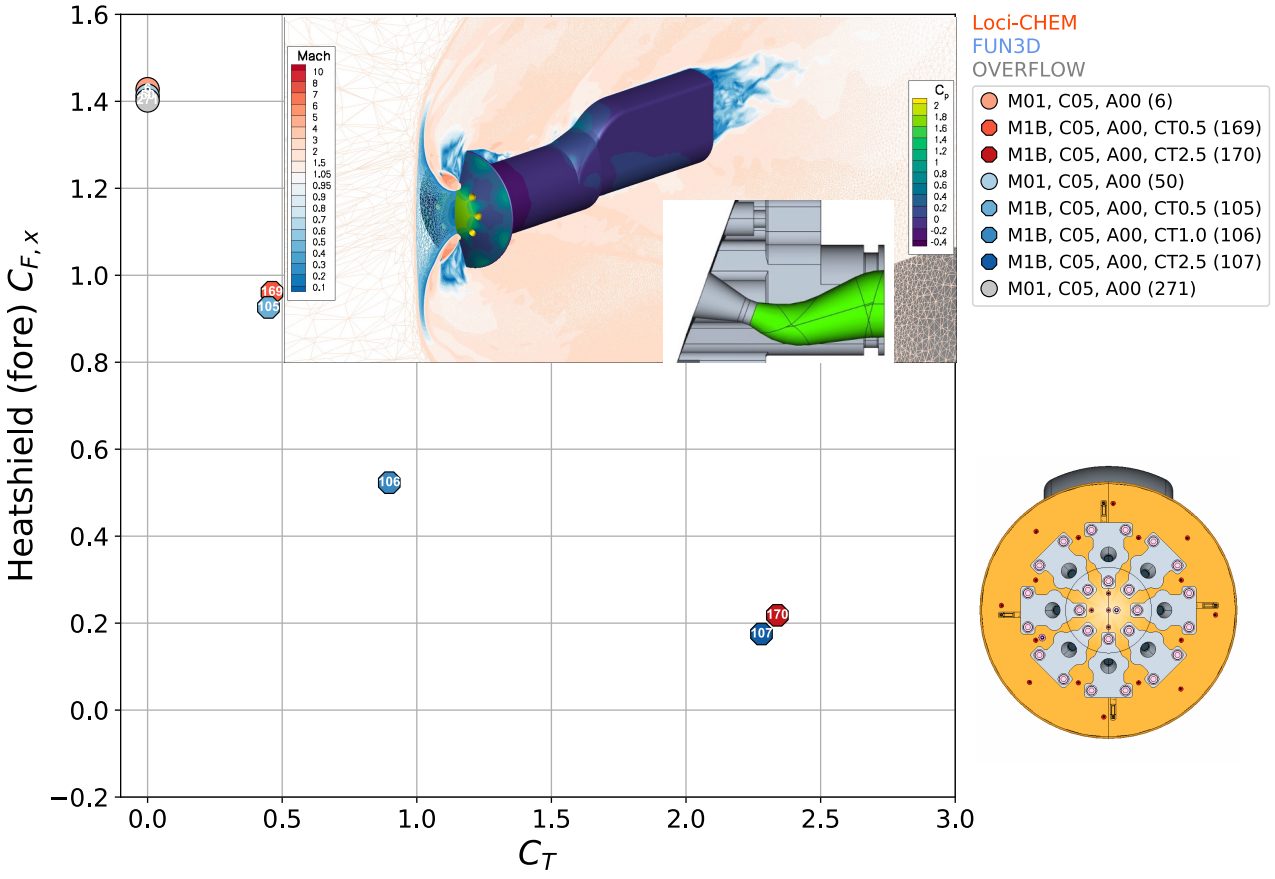

Model 1E at Condition 05 (AoA = 0)

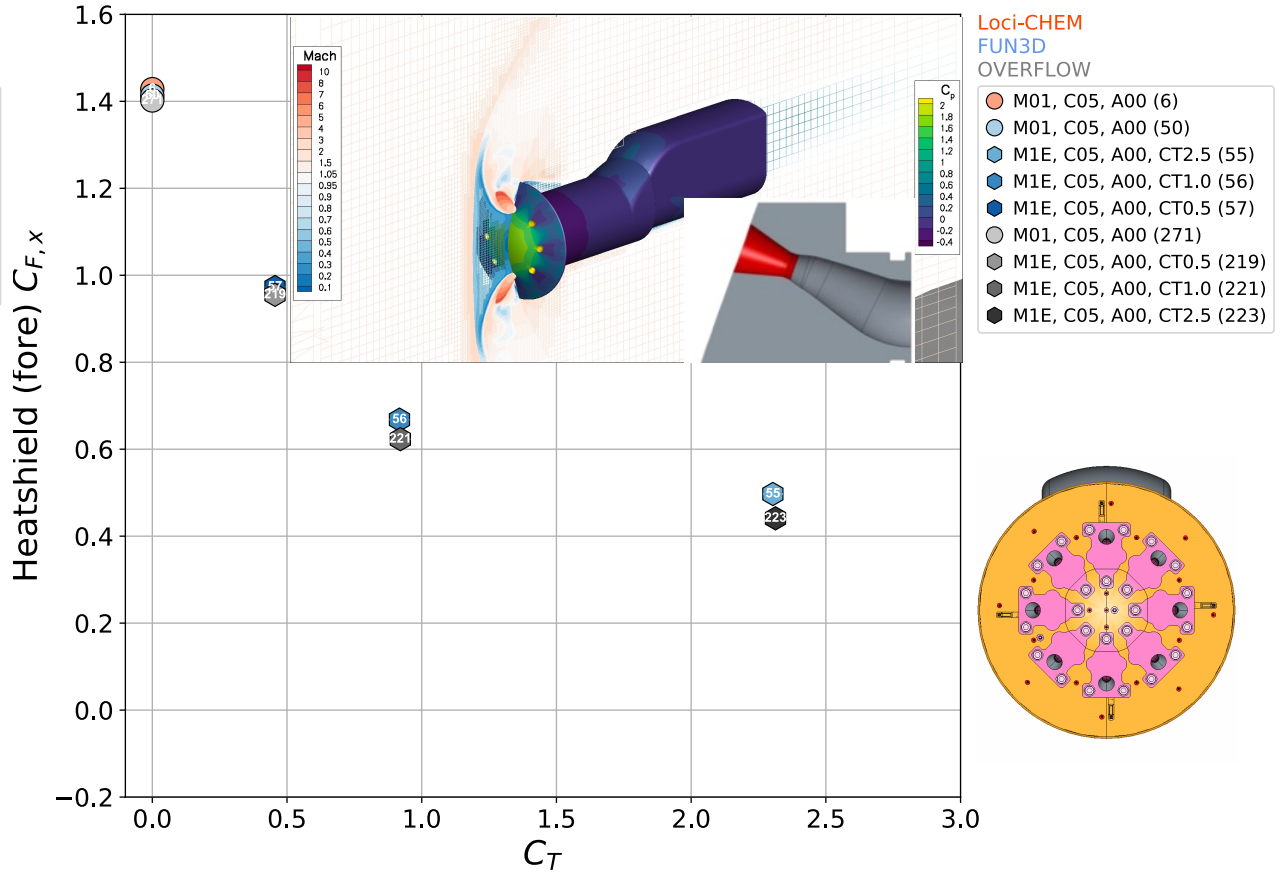

Summary

- A test will be run in the NASA Langley Research Center Unitary Plan Wind Tunnel in 2022 in order to investigate aerodynamic interference effects due to simulated (air) retrorocket nozzle plumes at supersonic freestream conditions
- The main test objective is to provide relevant data so that CFD predictive capabilities for retropropulsion can be assessed in a wind tunnel environment
- Two wind tunnel models have been designed and fabricated to be geometrically-scaled versions of the current flight reference vehicles
  - Different nozzle parameters will be explored for the Low-L/D model
- The test data will consist of:
  - Six-component forces & moments from custom flow-through balance
  - Steady and unsteady discrete surface pressures
  - Global steady surface pressure using pressure sensitive paint
  - High-speed schlieren video
  - New plume seeding technique
- To date, over 350 CFD solutions have been completed at planned test conditions, with trends matching expectations for two models with eight jets: blunt and slender
- The test will be followed by extensive uncertainty quantification and comparisons between the data and CFD predictions, both of which will be documented in the open literature

References

AIAA Paper 2022-0911

[1]Braun, R. D., and Manning, R. M., "Mars Exploration Entry, Descent, and Landing Challenges," *Journal of Spacecraft and Rockets*, Vol. 44, No. 2, 2007, pp. 310–323.

[2]Dwyer-Ciancolo, A. M., et al, "Entry, Descent and Landing Systems Analysis Study: Phase 1 Report," NASA TM 216720, National Aeronautics and Space Administration, July 2010.

[3]Dwyer-Ciancolo, A. M., et al, "Entry, Descent and Landing Systems Analysis Study: Phase 2 Report on Exploration Feed-Forward Systems," NASA TM 217055, National Aeronautics and Space Administration, February 2011.

[4]Edquist, K. T., Korzun, A. M., Dyakonov, A. A., Studak, J. W., Kipp, D. M., and Dupzyk, I. C., "Development of Supersonic Retropropulsion for Future Mars Entry, Descent, and Landing Systems," *Journal of Spacecraft and Rockets*, Vol. 51, No. 3, 2014, pp. 650–663.

[5]Cianciolo, A. D., and Polsgrove, T. T., "Human Mars Entry, Descent, and Landing Architecture Study Overview," AIAA Paper 2016-5494, September 2016.

[6]Cianciolo, A. D., and Polsgrove, T. T., "Human Mars Entry, Descent and Landing Architecture Study: Phase 2 Summary," AIAA Paper 2018-5191, September 2018.

[7]Cianciolo, A. D., Korzun, A., Edquist, K., Samareh, J., Sostaric, R., Calderon, D., and Garcia, J. A., "Human Mars Entry, Descent and Landing Architecture Study: Phase 3 Summary," AIAA Paper 2020-1509, January 2020.

[8]Berry, S. A., Rhode, M. R., and Edquist, K. T., "Supersonic Retropropulsion Validation Experiment in the NASA Langley Unitary Plan Wind Tunnel," *Journal of Spacecraft and Rockets*, Vol. 51, No. 3, 2014, pp. 664–679.

[9]Berry, S. A., Rhode, M. R., and Edquist, K. T., "Supersonic Retropropulsion Experimental Results from NASA Ames 9×7 Foot Supersonic Wind Tunnel," *Journal of Spacecraft and Rockets*, Vol. 51, No. 3, 2014, pp. 724–734.

[10]Zarchi, K. A., Schauerhamer, D. G., Kleb, W. L., Carlson, J.-R., and Edquist, K. T., "Analysis of Navier-Stokes Codes Applied to Supersonic Retropropulsion Wind–Tunnel Test," *Journal of Spacecraft and Rockets*, Vol. 51, No. 3, 2014, pp. 680–692.

[11]Schauerhamer, D. G. Zarchi, K. A., Kleb, W. L. Carlson, J.-R., and Edquist, K. T., "Supersonic Retropropulsion Computational Fluid Dynamics Validation with Langley 4x4 Foot Test Data," *Journal of Spacecraft and Rockets*, Vol. 51, No. 3, 2014, pp. 693–714.

[12]Schauerhamer, D. G. Zarchi, K. A., Kleb, W. L., and Edquist, K. T., "Supersonic Retropropulsion Computational-Fluid-Dynamics Validation with Ames 9x7 Foot Test Data," *Journal of Spacecraft and Rockets*, Vol. 51, No. 3, 2014, pp. 735–749.

[13]Braun, R. D., Sforzo, B., and Campbell, C., "Advancing Supersonic Retropropulsion Using Mars-Relevant Flight Data: An Overview," AIAA Paper 2017-5292, September 2017.

[14]Edquist, K. T., et al, "Comparison of Navier-Stokes Flow Solvers to Falcon 9 Supersonic Retropropulsion Flight Data," AIAA Paper 2017-5296, September 2017.

[15]Sforzo, B. and Braun, R. D., "Feasibility of Supersonic Retropropulsion Based on Assessment of Mars-Relevant Flight Data," AIAA Paper 2017-5295, September 2017.

[16]Korzun, A., Canabal, F., Tang, C., Childs, R., Van Norman, J., Tynis, J., and Bibb, K., "Powered Descent Aerodynamics for Low and Mid Lift-to-Drag Human Mars Entry, Descent and Landing Vehicles," AIAA Paper 2020-1510, January 2020.

[17]Ross, J. C., et al, "Evaluation of CFD as a Surrogate for Wind-Tunnel Testing for Mach 2.4 to 4.6 - Project Overview," AIAA Paper 2021-2961, August 2021.

[18]Edquist, K. T., Korzun, A. M., Kleb, B., Hawke, V. M., Rizh, Y. M., Olsen, M. E., Canabal, F., "Model Design and Pre-Test CFD Analysis for a Supersonic Retropropulsion Wind Tunnel Test," AIAA Paper 2020-2230, January 2020.

[19]Edquist, K. T., Alter, S. J., Glass, C. E., Kleb, W. L., Korzun, A. M., Wood, W. A., Childs, R. E., Halstrom, L. D., Matsuno, K. V., and Canabal, F., "Computational Modeling of Mars Retropropulsion Concepts Tested in the Langley Unitary Plan Wind Tunnel," AIAA Paper 2022-XXXX, January 2022.

[20]Halstrom, L. D., Pulliam, T. H., Childs, R. E., and Stremel, P. M., "OVERFLOW Analysis of Supersonic Retropropulsion Testing on a Blunt Mars Entry Vehicle Concept," AIAA Paper 2022-XXXX, January 2022.

[21]Matsuno, K. V., Childs, R. E., Stremel, P. M., Garcia, J. A., and Pulliam, T. H., "OVERFLOW Analysis of Supersonic Retropropulsion Testing on the CobraMRV Mars Entry Vehicle Concept," AIAA Paper 2022-XXXX, January 2022.

[22]Acharya, A. S., Lowe, K. Todd, Danehy, P. M., Edquist, K. T., Burns, R. A., and Pham, H. T., "Seeding Method for Velocimetry and Visualization of Supersonic Retropropulsion Nozzle Plumes," AIAA Paper 2022-XXXX, January 2022.

[23]Burns, D. E., Parker, P. A., Cagle, C. M., Hawke, V. M., Tor, K. G., and Kleb, B., "A New Flow-Through Wind Tunnel Balance for Retropropulsion Testing," AIAA Paper 2022-XXXX, January 2022.

[24]Rhode, M. N., et al, "Flow Characterization of the NASA Langley Unitary Plan Wind Tunnel, Test Section 2: Experimental Results," Aiaa presentation, August 2021.

[25]Hubbard, E. P., and Houlden, H. P., "Evaluation of CFD as a Surrogate for Wind-Tunnel Testing: Experimental Uncertainty Quantification for the UPWT Flow Survey Test," AIAA Paper 2021-2962, August 2021.

[26]Childs, R. E., et al, "Flow Characterization of the NASA Langley Unitary Plan Wind Tunnel, Test Section 2: Computational Results," AIAA Paper 2021-2963, August 2021.

[27]Korzun, A. M., and Cassel, L. A., "Scaling and Similitude in Single Nozzle Supersonic Retropropulsion Aerodynamics Interference," AIAA Paper 2020-0039, January 2020.

References

AIAA Paper 2022-0912

[1]Braun, R. D., and Manning, R. M., "Mars Exploration Entry, Descent, and Landing Challenges," *Journal of Spacecraft and Rockets*, Vol. 44, No. 2, 2007, pp. 310–323.

[2]Dwyer-Ciancolo, A. M., et al, "Entry, Descent and Landing Systems Analysis Study: Phase 1 Report," NASA TM 216720, National Aeronautics and Space Administration, July 2010.

[3]Dwyer-Ciancolo, A. M., et al, "Entry, Descent and Landing Systems Analysis Study: Phase 2 Report on Exploration Feed-Forward Systems," NASA TM 217055, National Aeronautics and Space Administration, February 2011.

[4]Edquist, K. T., Korzun, A. M., Dyakonov, A. A., Studak, J. W., Kipp, D. M., and Dupzyk, I. C., "Development of Supersonic Retropropulsion for Future Mars Entry, Descent, and Landing Systems," *Journal of Spacecraft and Rockets*, Vol. 51, No. 3, 2014, pp. 650–663.

[5]Cianciolo, A. D., and Polsgrove, T. T., "Human Mars Entry, Descent, and Landing Architecture Study Overview," AIAA Paper 2016-5494, September 2016.

[6]Cianciolo, A. D., and Polsgrove, T. T., "Human Mars Entry, Descent and Landing Architecture Study: Phase 2 Summary," AIAA Paper 2018-5191, September 2018.

[7]Cianciolo, A. D., Korzun, A., Edquist, K., Samareh, J., Sostaric, R., Calderon, D., and Garcia, J. A., "Human Mars Entry, Descent and Landing Architecture Study: Phase 3 Summary," AIAA Paper 2020-1509, January 2020.

[8]Berry, S. A., Rhode, M. R., and Edquist, K. T., "Supersonic Retropropulsion Validation Experiment in the NASA Langley Unitary Plan Wind Tunnel," *Journal of Spacecraft and Rockets*, Vol. 51, No. 3, 2014, pp. 664–679.

[9]Berry, S. A., Rhode, M. R., and Edquist, K. T., "Supersonic Retropropulsion Experimental Results from NASA Ames 9×7 Foot Supersonic Wind Tunnel," *Journal of Spacecraft and Rockets*, Vol. 51, No. 3, 2014, pp. 724–734.

[10]Zarchi, K. A., Schauerhamer, D. G., Kleb, W. L., Carlson, J.-R., and Edquist, K. T., "Analysis of Navier-Stokes Codes Applied to Supersonic Retropropulsion Wind–Tunnel Test," *Journal of Spacecraft and Rockets*, Vol. 51, No. 3, 2014, pp. 680–692.

[11]Schauerhamer, D. G. Zarchi, K. A., Kleb, W. L. Carlson, J.-R., and Edquist, K. T., "Supersonic Retropropulsion Computational Fluid Dynamics Validation with Langley 4x4 Foot Test Data," *Journal of Spacecraft and Rockets*, Vol. 51, No. 3, 2014, pp. 693–714.

[12]Schauerhamer, D. G. Zarchi, K. A., Kleb, W. L., and Edquist, K. T., "Supersonic Retropropulsion Computational-Fluid-Dynamics Validation with Ames 9x7 Foot Test Data," *Journal of Spacecraft and Rockets*, Vol. 51, No. 3, 2014, pp. 735–749.

[13]Edquist, K. T., Falman, B. E., Watkins, A. Neal, Burns, D. E., and Morr, D. E., "Testing of Mars Retropropulsion Concepts in the Langley Unitary Plan Wind Tunnel," AIAA Paper 2022-XXXX, January 2022.

[14]Halstrom, L. D., Pulliam, T. H., Childs, R. E., and Stremel, P. M., "OVERFLOW Analysis of Supersonic Retropropulsion Testing on a Blunt Mars Entry Vehicle Concept," AIAA Paper 2022-XXXX, January 2022.

[15]Matsuno, K. V., Childs, R. E., Stremel, P. M., Garcia, J. A., and Pulliam, T. H., "OVERFLOW Analysis of Supersonic Retropropulsion Testing on the CobraMRV Mars Entry Vehicle Concept," AIAA Paper 2022-XXXX, January 2022.

[16]Acharya, A. S., Lowe, K. Todd, Danehy, P. M., Edquist, K. T., Burns, R. A., and Pham, H. T., "Seeding Method for Velocimetry and Visualization of Supersonic Retropropulsion Nozzle Plumes," AIAA Paper 2022-XXXX, January 2022.

[17]Burns, D. E., Parker, P. A., Cagle, C. M., Hawke, V. M., Tor, K. G., and Kleb, B., "A New Flow-Through Wind Tunnel Balance for Retropropulsion Testing," AIAA Paper 2022-XXXX, January 2022.

[18]Rhode, M. N., et al, "Flow Characterization of the NASA Langley Unitary Plan Wind Tunnel, Test Section 2: Experimental Results," Aiaa presentation, August 2021.

[19]Childs, R. E., et al, "Flow Characterization of the NASA Langley Unitary Plan Wind Tunnel, Test Section 2: Computational Results," AIAA Paper 2021-2963, August 2021.

[20]Hubbard, E. P., and Houlden, H. P., "Evaluation of CFD as a Surrogate for Wind-Tunnel Testing: Experimental Uncertainty Quantification for the UPWT Flow Survey Test," AIAA Paper 2021-2962, August 2021.

[21]Korzun, A., Canabal, F., Tang, C., Childs, R., Van Norman, J., Tynis, J., and Bibb, K., "Powered Descent Aerodynamics for Low and Mid Lift-to-Drag Human Mars Entry, Descent and Landing Vehicles," AIAA Paper 2020-1510, January 2020.

[22]Nichols, R. H. and Buning, P. G., "User's Manual for OVERFLOW 2.3," February 2021.

[23]Rogers, S. E., Roth, K., Nash, S. M., Baker, M. D., Slotnick, J. P., Whitlock, M., and Cao, H. V.,, "Advances in Overset CFD Processes Applied to Subsonic High-Lift Aircraft," AIAA Paper 2000-4216, 2000.

[24]Chan, W. M., "The Overgrid Interface for Computational Simulations on Overset Grids," AIAA Paper 2002-3188, 2002.

[25]Chan, W. M., "Developments in Strategies and Software Tools for Overset Structured Grid Generation and Connectivity," AIAA Paper 2011-3051, 2011.

[26]Buning, P. G., and Pulliam, T. H., "Near-Body Grid Adaption for Overset Grids," AIAA Paper 2016-3326, 2016.

[27]Menter, F. R., "Two-Equation Eddy-Viscosity Turbulence Models for Engineering Applications," *AIAA Journal*, Vol. 32, No. 8, 1994, pp. 1598–1605.

[28]Spalart, P. R., "Strategies for turbulence modelling and simulations," *International Journal of Heat and Fluid Flow*, Vol. 21, No. 3, 2000, pp. 252–263.

[29]Mani, M., Babcock, D. A., Winkler, C. M., and Spalart, P. R., "Predictions of a Supersonic Turbulent Flow in a Square Duct," AIAA Paper 2013-860, January 2013.

[30]Nichols, R. H., "Algorithm and Turbulence Model Requirements for Simulating Vortical Flows," AIAA Paper 2008-337, 2008.

[31]Suzen, Y., and Hoffmann, K., "Investigation of Supersonic Jet Exhaust Flow by One- and Two-Equation Turbulence Models," AIAA Paper 1998-322, January 1998.

[32]Childs, R., et al, "Flow Characterization of the NASA Langley Unitary Plan Wind Tunnel, Test Section 2: Computational Results," AIAA Paper 2021-2963, 2021.

[33]Luke, E., and George, T., "Loci: A Rule-Based Framework for Parallel Multidisciplinary Simulation Synthesis," *Journal of Functional Programming*, Vol. 15, No. 3, May 2005, pp. 477–502.

[34]Luke, E., *A Rule-Based Specification System for Computational Fluid Dynamics*, Master's thesis, Mississippi State University, December 1999.

[35]Biedron, R. T., et al, "FUN3D Manual: 13.7," NASA TM 2020-5010139, Nov. 2020.

[36]Spalart, P. R, Deck, S., Shur, M. L., Squires, K. D., Strelets, M. Kh., and Travin, A., "A New Version of Detached-Eddy Simulation, Resistant to Ambiguous Grid Densities," *Theoretical and Computational Fluid Dynamics*, Vol. 20, No. 3, May 2006.

[37]Spalart, P. R., "Strategies for Turbulence Modeling and Simulations," *International Journal of Heat and Fluid Flow*, Vol. 21, No. 3, June 2000, pp. 252–263.

[38]Shur, M. L, Stretlets, M. K., Travin, A. K., Spalart, P. R., "Turbulence Modeling in Rotating and Curved Channels: Assessing the Spalart-Shur Correction," *AIAA Journal*, Vol. 38, No. 5, 2000, pp. 784–792.

[39]Vatsa, V. N., and Lockard, D. P., "Assessment of Hybrid RANS/LES Turbulence Models for Aeroacoustics Applications," AIAA Paper 2010-4001, June 2010.

[40]Van Leer, B., "Towards the Ultimate Conservative Difference Scheme. V. A Second-Order Sequel to Godunov's Method," *Journal of Computational Physics*, Vol. 32, No. 1, 1979, pp. 101–136.

[41]Kleb, W. L., Schoenenberger, M., Korzun, A. M., and Park, M. A., "Sketch-to-Solution: A Case Study in RCS Aerodynamic Interaction," AIAA Paper 2020-0673, January 2020.

Acknowledgments

- The wind tunnel model and test are funded under NASA's Aerosciences Evaluation and Test Capability program office
- Nicholas Marino and Donald Morr of Millennium Engineering and Integration Services completed the model designs for fabrication
- Veronica Hawke of Science and Technology Corporation prepared the geometries for grid generation software.
- Many of the CFD calculations have been, and will be, run on NASA Advanced Supercomputing Division computers
- CFD analysis to date has been funded by the NASA Space Technology Mission Directorate's Game Changing Development Program
- Thank you to Michael Park of NASA Langley Research Center for geometry and mesh adaptation support of the FUN3D solutions, and Kyle Thompson of NASA Langley for implementing the FUN3D boundary condition necessary for using specified tunnel inflow conditions